

2nd International UVSOR Workshop on Low-Energy Photoemission of Solids using Synchrotron Radiation (LEPES09)

October 3rd - 4th, 2009 [A Satellite Meeting of ICES 11, Nara, Japan]

INVITED SPEAKERS

Donglai FENG

Hojun IM

Akihiro INO

Chengyoung KIM

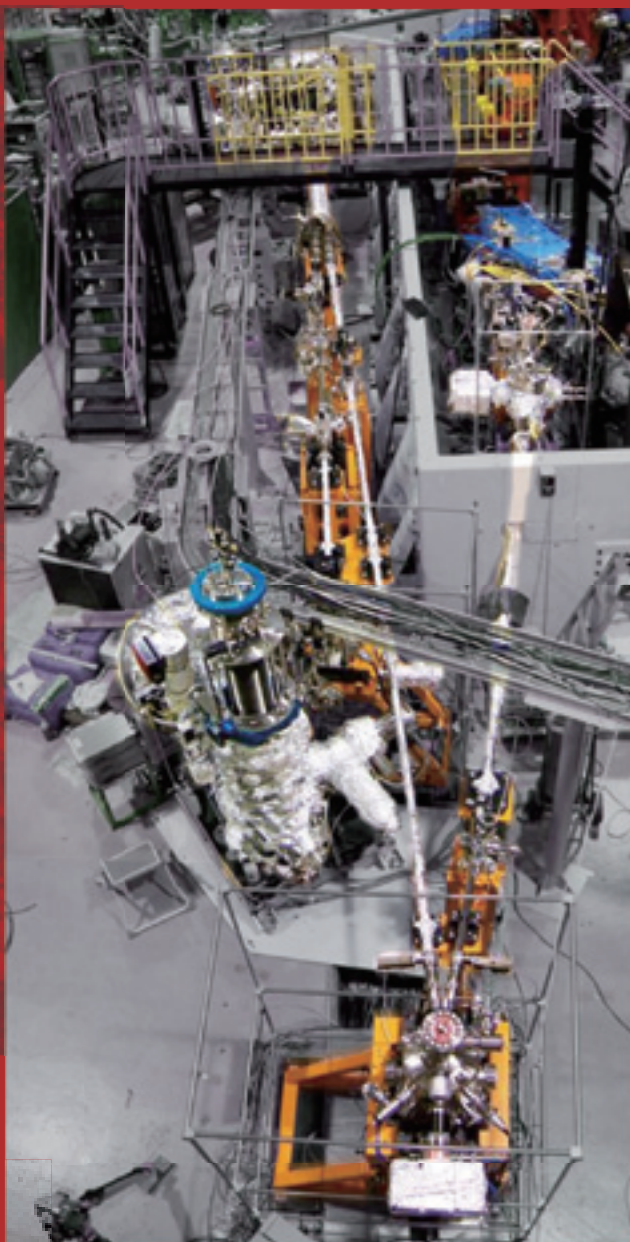
Takayuki KISS

Luca PETACCIA

Seigo SOUMA

Tsunehiro TAKEUCHI

Teppei YOSHIDA



UVSOR II
since 2003

PHOTOEMISSION SPECTROSCOPY OF SOLIDS
USING SYNCHROTRON RADIATION
RELATED SPECTROSCOPIC RESEARCH
OF LOW ENERGY ELECTRONIC STRUCTURE AND FERMILOGY
NEW INSTRUMENTS FOR PHOTOEMISSION SPECTROSCOPY
OF SOLIDS USING SYNCHROTRON RADIATION



Place:

Okazaki Conference Center, and UVSOR Facility,
Institute for Molecular Science

Contact Person:

Shin-ichi KIMURA [kimura@ims.ac.jp]

Program

October 3rd (Sat.)		
Place: Middle conference room (1st floor), Okazaki Conference Center, Okazaki, Japan		
15:00-	Registration.	
18:00-(20:00)	Get together party	
October 4th (Sun.)		
Place: Small conference room (2nd floor), Okazaki Conference Center		
9:00-9:10	S. Kimura (UVSOR)	Opening remark
1. Superconductors (Chair; T. Ito)		
9:10-9:35	D. Feng (Fudan Univ.)	Electronic structure of iron-based superconductors
9:35-10:00	T. Yoshida (Univ. Tokyo)	Two-gap behaviors of the high-T _c cuprate superconductors: Universal versus material-dependent properties
10:00-10:25	A. Ino (Hiroshima Univ.)	Low-energy ARPES study of novel multi-band superconductors at HiSOR
10:25-11:00	Coffee break + Group photo	
2. Oxides and theory (Chair; S. Suga)		
11:00-11:25	C. Kim (Yonsei Univ.)	Temperature dependent ARPES studies of Sr ₄ RuO ₄
11:25-11:50	L. Petaccia (Elettra)	Quasiparticles at the Mott transition in V ₂ O ₃ studied by bulk-sensitive VUV angle-resolved photoemission spectroscopy
11:50-12:15	K. Ji (KEK)	Quasiparticle dynamics and electron-phonon coupling in graphene
12:15-15:00	Lunch + Poster session + UVSOR site tour	
3. Functional materials (Chair; K. Soda)		
15:00-15:25	T. Takeuchi (Nagoya Univ.)	Role of coherent part and incoherent part in the electron transport properties of the materials characterized by strong electron correlation
15:25-15:50	H. J. Im (Hirosaki Univ.)	Systematic angle-resolved photoemission study of Ce-based heavy-fermion systems
15:50-16:15	T. V. Kuznetsova (Russian Academy of Science)	Electronic structure of CuIn ₅ Se ₈ studied by angle-resolved photoemission spectroscopy
16:15-16:45	Coffee break	
4. Low-energy PES using other sources (Chair; S. Kimura)		
16:45-17:10	T. Kiss (Univ. Tokyo)	Ultrahigh resolution laser-angle-resolved photoemission spectroscopy
17:10-17:35	S. Souma (Tohoku Univ.)	Development of bulk-sensitive spin-resolved ultrahigh-resolution photoemission spectrometer
17:35-	T. Ito (Nagoya Univ.)	Closing remark
18:30-(20:30)	Banquet at an Izakaya restaurant (Japanese pub)	
October 5th (Mon.)		
Move to Nara by public transportations.		

Poster presentation

01	K. Iwano (KEK)	Direct Domain Excitation by Photoemission and Its Dynamical Features Manifesting in ARPES spectra
02	Y. Takeichi (Univ. Tokyo)	Valence-band Electronic Structure of FeSi studied by high-resolution Angle-Resolved Photoelectron Spectroscopy (ARPES)
03	T. Hirahara (Univ. Tokyo)	A topological metal at the surface of an ultrathin BiSb alloy film
04	K. Soda (Nagoya Univ.)	Electronic Structure of Pseudo-one Dimensional $\text{Ba}_3\text{Co}_2\text{O}_6(\text{CO}_3)_{0.7}$
05	M. Imamura (Kobe Univ.)	Surface Chemistry of Butyl-Passivated Silicon Nanoparticles Studied by Synchrotron-Radiation Photoelectron Spectroscopy
06	K. Nakayama (Tohoku Univ.)	Low-energy angle-resolved photoemission spectroscopy of Fe-based high-Tc superconductor $\text{Ba}_{1-x}\text{K}_x\text{Fe}_2\text{As}_2$
07	T. Nakagawa (IMS)	Magnetic Circular Dichroism in Valence Band using Laser Excitation
08	J. Onoe (Tokyo Inst. Tech.)	In situ photoelectron spectra of an electron-beam irradiated C_{60} film
09	Y. Miyata (Ritsumeikan Univ.)	Electronic structure of $\text{Mn}_3\text{Cu}_{1-x}\text{Ga}_x\text{N}$ studied by soft X-ray photoelectron spectroscopy
10	V. I. Grebennikov (Russian Academy of Science)	"L+1 rule" for continuous electron-hole excitations in photoemission spectra
11	A. Sekiyama (Osaka Univ.)	Temperature and substitution dependence of extremely low-energy photoemission spectra on $\text{Sm}_{1-x}\text{Eu}_x\text{B}_6$
12	A. Taleb-Ibrahimi (SOLEIL)	ARPES and spin resolved Investigations on the 8-1500 eV high resolution Cassiopee beamline at SOLEIL
13	H. Miyazaki (UVSOR)	Temperature Dependent Angle-Resolved Photoemission Spectroscopy on Ferromagnetic EuO Thin Films
14	T. Ito (Nagoya Univ.)	Present status of VUV angle-resolved photoemission beamline BL7U at UVSOR-II
15	T. Ito (Nagoya Univ.)	Improvement of the SGM-TRAIN monochromator at UVSOR-II BL5U for low excitation-energy photoemission
16	M. Sakai (UVSOR)	Development of Integrated Software for Beamline Control for Photoemission Beamlines at UVSOR-II

Electronic structure of iron-based superconductors

Donglai Feng

Department of Physics, Fudan University, Shanghai, 200433, China

Iron based superconductors have ignited another round of intensive research on high temperature superconductivity. The electronic structure measured by angle resolved photoemission spectroscopy provides crucial information on the microscopic nature of this new class of superconductors.

In this talk I will discuss some of our recent works in this area.

(1) Multiple orbitals are considered a key feature of this new class of superconductors. With polarization-dependent photoemission and matrix element analysis, we were able to identify the orbital nature of various bands in the superconducting $\text{BaFe}_{2-x}\text{Co}_x\text{As}_2$ and $\text{FeTe}_x\text{Se}_{1-x}$ systems. Our results are rather different from the LDA calculations, indicative strong correlation effects.

(2) Anomalous band splittings in the spin density wave (SDW) state of the parent compounds have been observed, which leads to a novel SDW mechanism that does not require Fermi surface nesting in these materials.

(3) The isotropic superconducting gap around individual Fermi surfaces of $\text{Ba}_{1-x}\text{K}_x\text{Fe}_2\text{As}_2$ has been examined with various photon energies that sample different k_z 's.

[1] L. X. Yang et al. Phys. Rev. Lett. **102**, 107002 (2009).

[2] Y. Zhang et al. Phys. Rev. Lett. **102**, 127003 (2009).

[3] Y. Zhang et al. arXiv: cond-mat/0904.4022 (2009)

Two-gap behaviors of the high- T_c cuprate superconductors: Universal versus material-dependent properties

T. Yoshida¹, M. Hashimoto¹, K. Tanaka², N. Mannella², Z. Hussain³, Z.-X. Shen²,
A. Fujimori¹, M. Kubota⁴, K. Ono⁴, S. Komiya⁵, Y. Ando⁶, H. Eisaki⁷, S. Uchida¹

¹ *Department of Physics, University of Tokyo, Bunkyo-ku, Tokyo 113-0033, Japan*

² *Department of Applied Physics and Stanford Synchrotron Radiation Laboratory, Stanford University, Stanford, CA94305*

³ *Advanced Light Source, Lawrence Berkeley National Lab, Berkeley, CA 94720, USA*

⁴ *Photon Factory, Institute of Materials Structure Science, KEK, Tsukuba, Ibaraki 305-0801, Japan*

⁵ *Central Research Institute of Electric Power Industry, Komae, Tokyo 201-8511, Japan*

⁶ *The Institute of Scientific and Industrial Research, Osaka University, Ibaraki, Osaka 567-0047, Japan*

⁷ *National Institute of Advanced Industrial Science and Technology, Tsukuba 305-8568, Japan*

One of the central issues in the research of the high- T_c cuprates superconductors is whether the pseudogap is a distinct phenomenon from superconductivity or a gap due to local pairing or incoherent superconducting fluctuations above T_c . In the former scenario, a possible origin of the pseudogap is preformed Cooper pairs lacking phase coherence. In the latter scenario, the pseudogap is due to a competing order such as spin density wave, charge density wave, d-density wave, etc. It has been well known that the pseudogap in the anti-nodal ($\pi, 0$) region increases with underdoping as observed by angle-resolved photoemission spectroscopy (ARPES). However, the energy gap measured by other experimental methods such as Andreev reflection, which is more directly associated with superconductivity, exhibits opposite trend, that is, the gap decreases with underdoping, suggesting a different origin of the superconducting gap from the antinodal gap.

A recent ARPES study of $\text{Bi}_2\text{Sr}_2\text{Ca}_{1-x}\text{Y}_x\text{Cu}_2\text{O}_8$ (Bi2212) has revealed the presence of two distinct energy gaps in different regions of momentum space [1,2]. One is the antinodal region as mentioned above, and increases with underdoping. The other opens in the near-nodal region showing a coherent peak, and does not increase with underdoping. On the other hand, attempts have been made to understand the pseudogap within a single d -wave energy gap [3]. In such a single gap picture, preformed Cooper pairs are the most likely origin of the pseudogap.

Since the doping and temperature dependences of the energy gap would reveal the entangled two-gap behavior, we have investigated the energy gap of lightly- to optimally-doped LSCO by ARPES as a function of doping and temperature. In the present work, the momentum dependence of the gap clearly exhibits two-gap behavior as in the case of heavily underdoped Bi2212: the pseudogap Δ^* in the antinodal region and the d -wave like gap Δ_0 around

the node (Fig. 1). The doping dependence of the obtained parameter Δ_0 qualitatively explains the reduction of the T_c with underdoping. Furthermore, from comparison of the present results with those on Bi2212 and other cuprates with higher T_c 's, we have found that the magnitude of the Δ^* and the pseudogap temperature T^* is not appreciably material-dependent, suggesting that the pseudogap is properties of a single CuO_2 plane. On the other hand, the magnitude of the Δ_0 , which is proportional to the superconducting gap, is strongly material-dependent (CuO_2 layer number dependent) like T_c , suggesting that they are influenced by the effect of neighboring CuO_2 planes and block layers.

References

- [1] K. Tanaka *et al.*, Science **314**, 1910 (2006).
- [2] W. S. Lee *et al.*, Nature **450**, 81 (2007).
- [3] A. Kanigel *et al.*, Nature Physics **2**, 447 (2006)

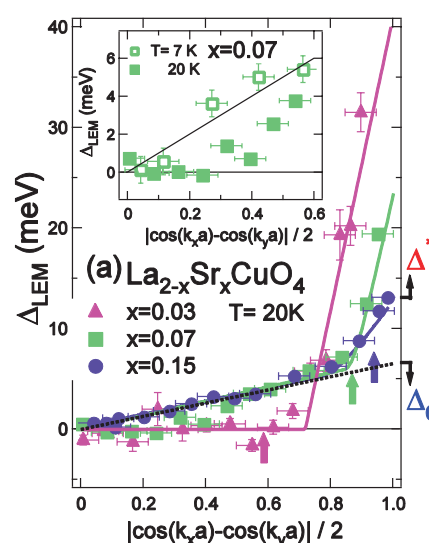


Fig. 1. Angular dependence of the gap of LSCO observed by ARPES. The definition of Δ^* and Δ_0 is shown for $x=0.15$.

Low-energy ARPES study of novel multi-band superconductors at HiSOR

A. Ino¹¹Graduate School of Science, Hiroshima University, Higashi-Hiroshima 739-8526, Japan

For understanding the mechanism of novel high-T_c superconductivity, the resolution of multiple sheets of Fermi surfaces is important issue. In bilayer cuprates, which are empirically known to have higher T_c than single-layered systems, two sheets of Fermi surfaces are present in close proximity due to small hybridization between two adjacent CuO₂ layers. In iron-based superconductors, all of five Fe 3d orbitals are responsible for low-energy electronic states, and more than three sheets of Fermi surfaces have been observed so far.

Using low-energy synchrotron radiation as the excitation photons of angle-resolved photoemission (ARPES), in general, the momentum- and energy-resolution become higher, the probing depth increases, and the perpendicular-momentum selectivity increases.

Bilayer cuprate, Bi₂Sr₂CaCu₂O_{8+δ} (Bi2212), has been studied by low-energy ARPES. We have found that the spectral-intensity ratio of a bonding band to an antibonding band drastically changes from 0% to 70% as a function of excitation photon energy due to the effect of transition matrix elements, and thus resolved the quasiparticle properties of two bilayer states. The nodal scattering rate is higher for antibonding band than for the bonding band in superconducting phase, indicating that the quasiparticles are scattered by the inhomogeneity of the potential from out-of-plane dopant oxygens. The magnitude of the superconducting gap is almost identical between the bonding and antibonding bands as shown in Fig. 1. With decreasing hole concentration, near-nodal superconducting gap region shrinks in momentum space for both of the bilayer bands. The width of bilayer splitting is narrower for the underdoped sample, showing the increase in two-dimensionality of electronic structure. This result is consistent with transport experiments.

Iron-based system, BaFe₂As₂ has been studied by a combination of low-energy ARPES at BL9A and polarization-dependent ARPES at BL1 in HiSOR. The orbital characters of low-energy bands have been determined from perpendicular-momentum dependence and polarization dependence. As shown in Fig. 2, the inner Fermi surface around Γ -Z axis shows strong dispersion in k_z direction, so that the Fermi-surface nesting is weak for the undoped material. Our results show that the top of this hole pocket comes down below the Fermi level at $k_z=0$, and that even- and odd-parity bands are degenerate at Γ point. Therefore, the inner Fermi surface is attributed to d_{xz} and d_{yz} orbitals.

This work was done in collaboration with H. Anzai, T. Fujita, Y. Nakashima, G. Hara, M. Arita, H. Namatame, M. Taniguchi, A. Fujimori, Z.-X. Shen, M. Ishikado, K. Fujita, S. Uchida, K. Kihou, C. H. Lee, H. Eisaki, A. Iyo, H. Kito, I. Hase, Y. Aiura.

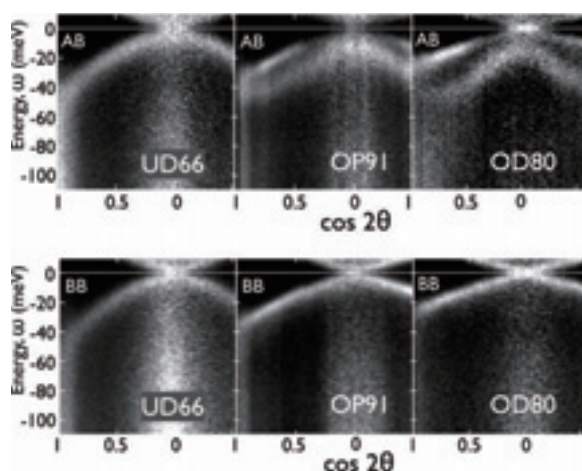


Fig. 1. ARPES spectral image taken along the antibonding-band (AB) and bonding-band (BB) Fermi surfaces of Bi₂Sr₂CaCu₂O_{8+δ} in superconducting phase (T = 10 K).

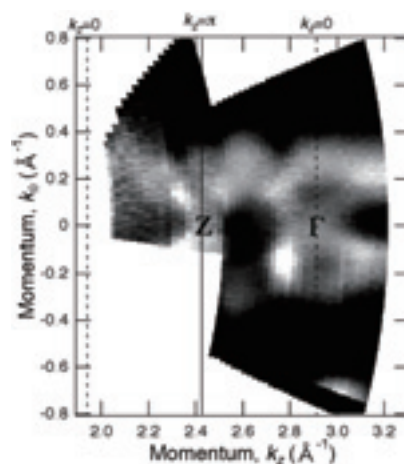


Fig. 2. ARPES spectral image taken along Γ -Z axis, a direction perpendicular to surface, for BaFe₂As₂.

Temperature dependent ARPES studies of Sr₂RuO₄

Chul Kim^{1*}, S. R. Park¹, C. S. Leem¹, D. J. Song¹, Y. K. Kim¹, S. K. Choi¹, W. S. Jung¹, Y. Y. Ko¹, H. Y. Choi¹, W. S. Kyung¹, G. R. Han¹, Y. Yoshida², R. G. Moore³, C. Kim¹

¹ Institute of Physics and Applied Physics, Yonsei University, Korea

² Nanoelectronics Research Institute, National Institute of Advanced Industrial Science and Technology, Japan

³ Stanford Synchrotron Radiation Lightsource, SLAC National Accelerator Laboratory, USA

Discovery of spin triplet superconductivity in Sr₂RuO₄ brought attention to the electronic structure studies on the system, especially by using angle resolved photoemission (ARPES). There are three bands that cross the Fermi level. The system is particularly interesting because these bands have different orbitals with different characters such as dimensionality. Along the way, it was found that there are surface states due to RuO₆ octahedral rotation on the surface layer, which results in a dramatic change in the electronic structure.

So far, only static properties of Sr₂RuO₄ have been studied by ARPES. To investigate the dynamic properties of Sr₂RuO₄ in the electronic structure, we have performed temperature dependent ARPES studies on Sr₂RuO₄ as well as LEED IV experiments. We found that there is very strong temperature dependence in the surface electronic structures. While 10K data show very strong surface states, raising temperature practically kills the surface state signal (figure 1). Surprisingly, the states are recovered when the samples are cooled back down to lower temperature.

To investigate the possible role of the structural change, we performed temperature dependent LEED IV experiment. The indication is that there is not much structural change in the surface atomic structure. This suggest that disappearance of the surface ARPES signal comes from dynamic fluctuation in the octahedral rotation. We will discuss the result in terms of possible quantum critical point.

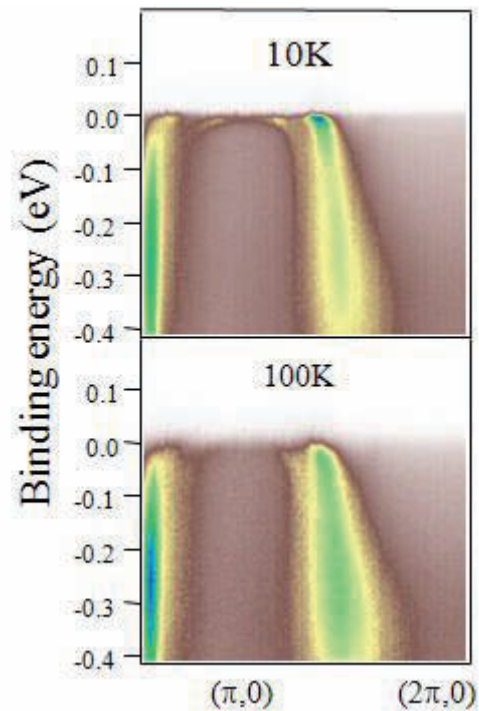


Fig. 1. Temperature dependent ARPES data from Sr₂RuO₄. The flat band near ($\pi,0$) is from the surface states.

Quasiparticles at the Mott transition in V_2O_3 studied by bulk-sensitive VUV angle-resolved photoemission spectroscopy

L. Petaccia¹, F. Rodolakis^{2,3}, B. Mansart², E. Papalazarou⁴, S. Gorovikov¹, P. Vilmercati¹, A. Goldoni¹, J. P. Rueff³, S. Lupi⁵, P. Metcalf⁶ and M. Marsi²

¹*Sincrotrone Trieste S.C.p.A., Strada Statale 14 Km 163.5, I-34149 Trieste, Italy*

²*Laboratoire de Physique des Solides, CNRS-UMR 8502, Université Paris-Sud, F-91405 Orsay, France*

³*Synchrotron SOLEIL, L'Orme des merisiers, Saint-Aubin BP 48, F-91192 Gif-sur-Yvette, France*

⁴*Laboratoire d'Optique Appliquée, ENSTA–Ecole Polytechnique, F-91761 Palaiseau, France*

⁵*CNR-INFN COHERENTIA and Dipartimento di Fisica, Università di Roma “La Sapienza”, Piazzale Aldo Moro 2, I-00185 Roma, Italy*

⁶*Department of Chemistry, Purdue University, West Lafayette, Indiana 47907, USA*

Understanding the electronic properties of quasiparticles in strongly correlated materials is the key to answer many important open questions in condensed matter physics. Angle resolved photoemission spectroscopy (ARPES) is one of the main experimental techniques to study this problem, but its intrinsic surface sensitivity often turns out to be a problem for the fermiology of coherent electronic states.

The BaD EIPh beamline at the Elettra synchrotron light source was constructed to perform ARPES at low photon energy, thus in a more bulk sensitive way, in conditions of high flux and high energy resolution [1]. These characteristics were exploited to explore the electronic properties of the prototype Mott compound V_2O_3 .

We found that spectral features corresponding to the quasiparticle peak in the metallic phase present a marked wave vector dependence, with a stronger intensity along the ΓZ direction. The analysis of their intensity for different probing depths shows the existence of a characteristic length scale for the attenuation of coherent electronic excitations at the surface. This length scale, which is larger than the thickness of the surface region as normally defined for noncorrelated electronic states, is found to increase when approaching the Mott transition [2]. These results are in agreement with the behavior of quasiparticles at surfaces as predicted by a very recent theoretical work [3], and appear to be of general interest also for other strongly correlated materials [4].

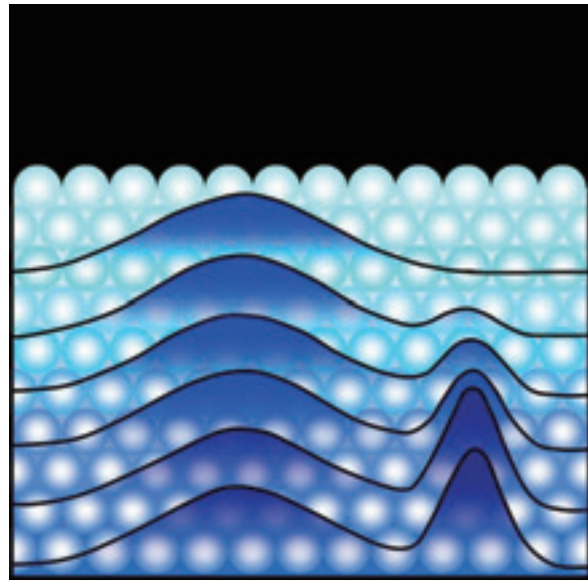


Fig. 1. In the V_2O_3 prototype Mott compound an insulating layer is present in a region near the surface even when the bulk is still a metal [4].

[1] L. Petaccia, P. Vilmercati, S. Gorovikov, M. Barnaba, A. Bianco, D. Cocco, C. Masciovecchio and A. Goldoni, *Nucl. Instr. and Meth. A* **606** (2009) 780.

[2] F. Rodolakis, B. Mansart, E. Papalazarou, S. Gorovikov, P. Vilmercati, L. Petaccia, A. Goldoni, J. P. Rueff, S. Lupi, P. Metcalf and M. Marsi, *Phys. Rev. Lett.* **102** (2009) 066805.

[3] G. Borghi, M. Fabrizio and E. Tosatti, *Phys. Rev. Lett.* **102** (2009) 066806.

[4] Synopsis in “Physics”:

<http://physics.aps.org/synopsis-for/10.1103/PhysRevLett.102.066805>

Quasiparticle dynamics and electron-phonon coupling in graphene

K. Ji, K. Iwano and K. Nasu

*Solid State Theory Division, Institute of Materials Structure Science, KEK
Graduate University for Advanced Studies, Oho 1-1, Tsukuba, Ibaraki 305-0801, Japan*

Graphene and graphite are important mother systems for carbon-based materials such as carbon nanotube and fullerene. Insight into these materials to understand the role of electron-phonon (e-ph) interaction has been attracting considerable research interests. Recently, experiments of high resolution angle-resolved photoemission spectroscopy (ARPES) are performed on graphite, and a sharp quasiparticle (QP) peak is observed at the Fermi surface (E_F). However, up to now, it is still puzzling and controversial that whether this sharp QP peak is due to a strong e-ph interaction or not [1,2].

In order to reveal the nature of this QP peak, we theoretically study the ARPES of a monolayer graphene by using quantum Monte Carlo simulation method. Our calculation confirms that a well-defined sharp QP peak arises at E_F , as shown in Fig. 1(c). But intensity of this peak decreases dramatically with the increase of e-ph coupling strength S . Furthermore, an energy gap may open at E_F provided large coupling S , justifying that the e-ph interaction in graphene cannot be very strong. In connection with ARPES, we have also intensively investigated the relation between QP dynamics and e-ph interaction, electronic states and doping level in graphene.

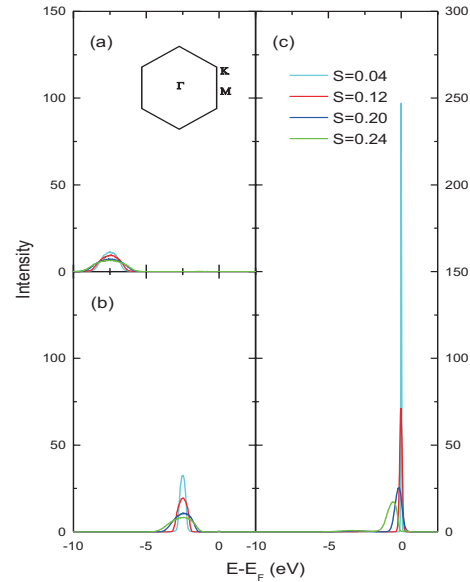


Fig. 1. Calculated ARPES intensity for graphene at (a) Γ , (b) M , and (c) K points under given e-ph coupling constants S . Inset of (a) shows Brillouin zone.

- [1] K. Sugawara, T. Sato, S. Souma, T. Takahashi, and H. Suematsu, *Phys. Rev. Lett.* **98** (2007) 036801.
- [2] C. S. Leem, B. J. Kim, Chul Kim, S. R. Park, T. Ohta, A. Bostwick, E. Rotenberg, H.-D. Kim, M. K. Kim, H. J. Choi, and C. Kim, *Phys. Rev. Lett.* **100** (2008) 016802.

Role of coherent part and incoherent part in the electron transport properties of the materials characterized by strong electron correlation

Tsunehiro Takeuchi

¹*EcoTopia Science Institute, Nagoya University, Nagoya 464-8603, Japan*

Recent progress in angle resolved photoemission spectroscopy (ARPES) allows us to gain deep insight into the momentum dependent electronic structure of the materials. The self-energy of quasiparticles can be also investigated by ARPES as a function of energy and momentum, in which information about the variety of many body effects including the electron correlations is involved. The real part of the self-energy indicates the energy shift from that of the bare electrons free from the many body effects, while the imaginary part represents the lifetime of the quasiparticles. A large number of groups including us have employed this highly sophisticated experimental technique to investigate the electronic structure and the many body effects of materials, such as the high- T_c superconductors.

We realized by using ARPES measurements that the electron transport properties could be quantitatively analyzed, because all factors, the number of electrons at a given energy, momentum dependent group velocity, and momentum dependent relaxation time, are obtainable from the ARPES measurements, provided that the lifetime of the quasiparticles is considered as the relaxation time of conducting wave packets. For the high- T_c superconductors, in which almost of all quasiparticles behave as a coherent wave, this method worked well and the electrical resistivity, thermoelectric power, and Hall coefficient were quantitatively reproduced by calculation using the information obtained from the ARPES measurement. [1]

The layered cobalt oxide Na_xCoO_2 is widely known to possess variety of unusual properties, such as superconductivity, the large magnitude of thermoelectric power, the Curie-Weiss magnetic susceptibility behavior coexisting together with the metallic electrical conduction, the charge density wave oriented insulating phase, and the spin density wave behaviors. Those characteristics are presumably caused by the strong electron correlation. Recently, we have intensively investigated the effect of strong electron correlation upon the electronic structure and the electron transport properties of Na_xCoO_2 by using high-resolution ARPES measurements, and found that the incoherent part as well as the coherent part, strongly affects the electron transport properties.

The electronic structure of layered cobalt oxides, including the present material Na_xCoO_2 , is characterized by the simultaneous possession of coherent part and incoherent part shown as Fig.1. Generally speaking, the incoherent part is caused by the strong electron correlation, and this strong

electron correlation drastically reduces the energy-width of the “coherent band”. Indeed, the observed energy-width of the “coherent band” is reduced to 1/3 of that of the band calculated by the FLAPW-LDA method. Note here that these characteristics in electronic structure cannot be predicted by the first principle calculation using the mean field theory. The use of the high-resolution ARPES, therefore, is of great importance in order to reveal the electronic structure of materials under the strong many body effects.

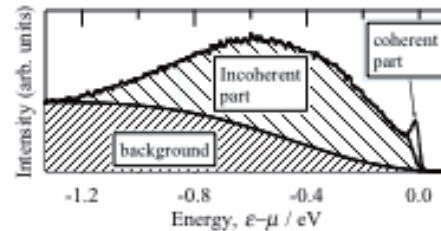


Fig. 1. An energy distribution curve of the $\text{Na}_{0.7}\text{CoO}_2$ at a Fermi wave vector. The spectrum is definitely characterized by the coherent and incoherent parts.

The temperature dependence of the thermoelectric power and the electrical resistivity was well accounted for with the Boltzmann transport theory provided that the contributions of coherent and incoherent part are properly taken into account. Both properties are dominantly determined by the coherent part at low temperature below 150 K and by the incoherent part at high temperature above 300K, respectively. The measured and calculated thermoelectric power of $\text{Na}_{0.7}\text{CoO}_2$ is shown in Fig.2 as one of the typical examples.

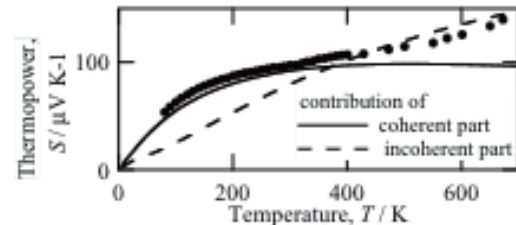


Fig. 2. Measured (markers) and calculated (lines) thermoelectric power of $\text{Na}_{0.7}\text{CoO}_2$.

[1] T. Kondo *et al.*, Phys. Rev. B **72** (2005) 024533., T. Kondo *et al.*, Phys. Rev. B **74** (2006) 225411., T. Kondo *et al.*, J. Elec. Spec. Relat. Phenom. **144-147** (2005) 1249-1252., T. Takeuchi *et al.*, J. Elec. Spec. Relat. Phenom. **156-158** (2007) 452-456., H. Komoto and T. Takeuchi, J. Elec. Mater. **38** (2009) 1365-1370.

Systematic angle-resolved photoemission study of Ce-based heavy-fermion systems

H. J. Im,¹ H. Miyazaki,² T. Ito,³ S. Kimura,^{2,4} K. E. Lee,⁵ Y. S. Kwon,⁵
A. Yasui,⁶ and H. Yamagami^{6,7}

¹ *Department of Advanced Physics, Hirosaki University, Hirosaki 036-8561, Japan*

² *UVSOR Facility, Institute for Molecular Science, Okazaki 444-8585, Japan*

³ *Graduate School of Engineering, Nagoya University, Nagoya 464-8603, Japan*

⁴ *School of Physical Sciences, The Graduate University for Advanced Studies, Okazaki 444-8585, Japan*

⁵ *Department of Physics, Sungkyunkwan University, Suwon 440-746, Korea*

⁶ *Synchrotron Radiation Research Center, Japan Atomic Energy Agency, SPring-8, Sayo, Hyogo 679-5148, Japan*

⁷ *Department of Physics, Kyoto Sangyo University, Kyoto 603-8555, Japan*

We present the systematic angle-resolved photoemission (ARPES) studies of Ce-based heavy fermion compounds, $\text{CeNi}_{1-x}\text{Co}_x\text{Ge}_2$, whose ground states are change from antiferromagnetic to non-magnetic heavy fermion via quantum critical point (QCP). Recently, it was clearly observed that the Kondo resonance (KR) peaks (Ce $4f^1$ state) are dispersed from above the Fermi-level (E_F) and cross E_F forming the diamond-shaped Fermi-surface (FS) in non-magnetic heavy-fermion system, $\text{CeCoGe}_{0.8}\text{Si}_{1.2}$ [1]. The systematic Ce $4d$ - $4f$ resonant ARPES studies of $\text{CeNi}_{1-x}\text{Co}_x\text{Ge}_2$ reveal that such momentum-dependence of KR peaks exists across QCP, indicating the itinerant character of f -electrons in agreement with the results of angle-integrated photoelectron spectroscopy [2].

References:

- [1] H. J. Im et al., Phys. Rev. Lett. **100**, 176402 (2008).
[2] H. J. Im et al., Phys. Rev. B **72**, 220405 (2005).

Electronic structure of CuIn_5Se_8 studied by angle-resolved photoemission spectroscopy

T.V. Kuznetsova¹, V.I. Grebennikov¹, C. Taubitz², M. Neumann²,
M.V. Yakushev³, M.V. Kuznetsov⁴

¹ *Institute of Metal Physics, UB RAS, 620041 Ekaterinburg, Russia*

² *Dortmund, DELTA, University of Osnabrück, D-49069 Osnabrück, Germany*

³ *Strathclyde University, G4 0NG Glasgow, United Kingdom*

⁴ *Institute of Solid State Chemistry, UB RAS, 620990 Ekaterinburg, Russia*

CuInSe_2 and related chalcopyrite compounds are recently attracting much attention due to potential applications for thin-film solar cells. Conversion efficiencies up to 19% for solar cells based on polycrystalline CuInSe_2 layers have been reached despite a lack of detailed information on material properties. Indium-rich compounds such as ordered defect compound CuIn_5Se_8 and CuIn_3Se_5 on surface of CuInSe_2 in the typical $\text{CdS}/\text{CuInSe}_2$ heterojunction play an important role for photovoltaic application due to their outstanding photoelectric characteristics [1]. However, the electronic structure of the compound CuIn_5Se_8 and the mechanism of strong localization of the states with the energies close to the Fermi level remained obscure. Knowledge on the stable surface structures of Cu chalcopyrites is very limited due to the difficulties in preparing clean well defined surfaces [2]. The electronic structure of the single crystal CuIn_5Se_8 surface has been investigated by angle-resolved photoelectron spectroscopy (ARPES) and x-ray photoemission spectroscopy (XPS). The samples were cleaved in ultrahigh vacuum of the analyzer chamber. Data have been collected for three different values of the incoming photon energy $h\nu = 20, 25,$ and 30 eV. We found that ARPES spectra along two different high symmetry directions in reciprocal space show existence of four bands. They are situated from 0 to 8 eV below the Fermi energy and have flat dispersions indicating a considerable localization of the electron states. In order to determine the chemical state of the surface and binding energy of the each core-level CuIn_5Se_8 the x-ray photoemission spectroscopy was performed using Al K_α radiation. The shape of valence-band spectra strongly depends on the exciting photon energies.

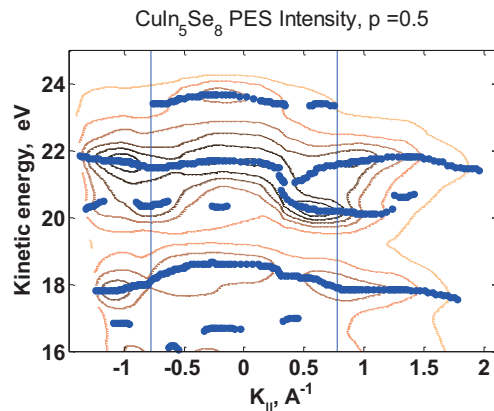


Fig. 1. The diagram of photoemission intensity as functions two variable: a wave vector (parallel a surface, along ΓM direction) and kinetic energy. Greasy curve - the coordinates of maxima of intensity on variable \AA , correspond to the law of dispersion of strips. The vertical lines show borders of the first Brillouin zone.

References:

- [1] S. Lany and A. Zunger, Phys. Rev. Lett., 100, 016401 (2008)
- [2] Th. Deniozou, N. Esser, Th. Schulmeyer, R. Hunger, Applied Phys. Lett., 88, 052102 (2006)

Ultrahigh resolution laser-angle-resolved photoemission spectroscopy

T. Kiss¹, K. Ishizaka^{1,2} and S. Shin^{1,2}

¹*Institute for Solid State Physics (ISSP), University of Tokyo, Kashiwa, Chiba 277-8581, Japan*

²*CREST, Japan Science and Technology Corporation (JST), Kashiwa, Chiba 277-8581, Japan*

It is well known that the variety of properties that conducting materials display stems from the electronic structure at and near the Fermi level (E_F). One of the most fascinating examples is superconductivity, in which pairing of two electrons makes a tiny energy gap at E_F , leading to unexpected physical properties. Angle-resolved photoemission spectroscopy (ARPES) is a very powerful method to measure electronic structure at and below E_F as it can provide the energy (ω) and momentum (k) resolved spectral function $A(k, \omega)$ of a solid. ARPES can thus measure band dispersions and Fermi surface topology as a function of temperature (T). [1] It has contributed significantly to our understanding of the electronic structure of solids. In the angle-integrated version also, PES has given us valuable results allowing comparisons with other techniques which probe the one-electron removal function, such as tunneling spectroscopy. Since the discovery of high- T_c superconductors, ARPES studies have followed a remarkable progress in energy and momentum resolution, driven by the purpose of determining the superconducting gap symmetry. These studies have usually employed synchrotron radiation or gas discharge lamps as a photon source coupled to a photoemission spectrometer, and for high energy resolution achieved using a He discharge lamp (He I : 21.218 eV). PES is also usually considered to be very surface sensitive as tunneling spectroscopy, it is well-known that the escape depth of photoelectrons show strong kinetic-energy dependence : it is highly surface sensitive for kinetic energies between 20- 50 eV, but can be made more bulk sensitive by changing the kinetic energy to very low and very high energies. [2] This can be done by simply changing the incident photon energy. Consequently, the increase of escape depth using soft-x rays ($h\nu \sim 1000$ eV) has been demonstrated with a resolution of ~ 100 meV. [3] This energy resolution is good enough to study the overall electronic structure but is about 100 times larger than, for example, the SC gap energy scale of a low- T_c superconductor, typically less than 1 meV. The energy resolution using synchrotron radiation with 20-30 eV photon energy is ~ 5 meV (recently ~ 2 meV below 10eV photon energy) for solid-state studies, which is again not enough for studying very low energy scale low temperature electronic structures. While PES using a He I resonance line (21.2 eV) can produce a ~ 1 -2 meV resolution, the escape depths using a photon energy of ~ 20 eV are less than 10 Å. This may not be suitable for studying materials having a surface electronic structure

completely different from the bulk, as is known for some correlated-electron systems.

To achieve the ultrahigh energy-momentum resolution and high bulk sensitivity, we have developed a low-temperature ultrahigh resolution system for polarization dependent ARPES using a vacuum ultra-violet (VUV) laser ($h\nu = 6.994$ eV) as a photon source. With the aim of addressing low energy physics, we show the system performance with angle-integrated PES at the highest energy resolution of 360 μ eV and the lowest temperature of 2.9 K. [4] At present, we have been achieved 150 meV of energy resolution and 1.8 K of lowest temperature in advanced 7 eV laser ARPES system. These new photoemission systems demonstrate that the ultrahigh resolution ARPES is quite important to understand electronic property of materials.

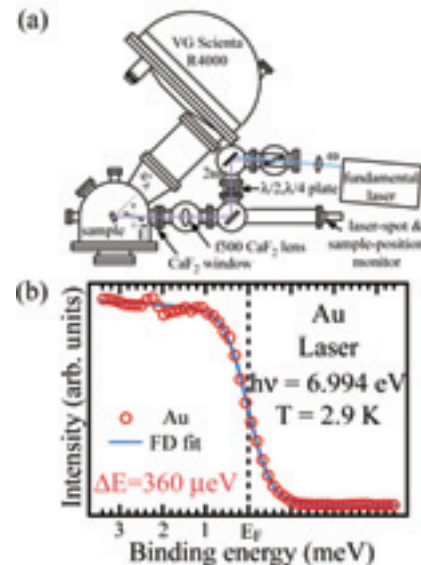


Fig. 1. (a) Schematic diagram of the LPES system. (b) Ultrahigh-resolution PES spectrum of an evaporated gold film measured at 2.9 K (red circles), together with the FD function at 2.9 K convolved by a Gaussian with full width at half maximum of 360 μ eV (a blue line).

[1] A. Kaminski *et al.*, Nature **416**, 610 (2002).

[2] M.P. Seah and W.A. Dench, Surface. Interface. Anal. **1**, 2 (1979).

[3] A. Sekiyama *et al.*, Nature **403**, 396 (2000).

[4] T. Kiss *et al.*, Rev. Sci. Instrum. **79**, 023106 (2008).

Development of bulk-sensitive spin-resolved ultrahigh-resolution photoemission spectrometer

S. Souma¹, A. Takayama², K. Sugawara², T. Sato² and T. Takahashi^{1,2,3}

¹WPI-AIMR, Tohoku University, Sendai 980-8578, Japan

²Department of Physics, Tohoku University, Sendai 980-8578, Japan

³Japan Science and Technology Agency, CREST, Kawaguchi 332-0012, Japan

Angle-resolved photoemission spectroscopy (ARPES) is known as a powerful technique to investigate the fine electronic structure relevant to the intriguing physical phenomena in solids such as superconductivity, heavy fermions, metal-insulator transition, and so on. This technique, yet, has suffered from two inherent problems originating in the principle of PES itself, namely, (1) the high surface sensitivity, and (2) the difficulty in resolving the spin polarization of electrons. To overcome those problems, we have constructed an ultrahigh resolution photoemission spectrometer equipped with a newly developed xenon-plasma discharge lamp and a mini-Mott detector.

Figure 1 shows the xenon plasma discharge lamp that provides several intense resonance lines from xenon plasma in the energy range of 8-11 eV, which is enough to achieve high bulk-sensitivity.[1] The energy width of radiation from the lamp is intrinsically very narrow owing to small Doppler broadening due to the high mass of the xenon atom, and low pressure operation of the discharging plasma reducing the self absorption effect. Combined with a large hemispherical energy analyzer and a spherical concaved grating, we achieved high energy resolution less than 1 meV as a total system in the spin-integrated mode. The photoelectron intensity excited by the xenon lamp is bigger than that of the ordinary helium lamps by 1-2 order of magnitude. This is quite useful to compensate the low efficiency in the case of spin-resolved photoemission.

We have developed a compact Mott spin detector operating at 25 kV and adapted it to the large hemispherical electron energy analyzer through an electron deflector lens. We have redesigned the analyzer and mounted the entrance of the deflector lens at a location close to the $\phi 40\text{mm}$ microchannel plate (MCP). This enables the observation of electron energy and momentum by the MCP with comparable quality to modern electron analyzers, simultaneously to the electron spin measurement by the Mott detector.

Figure 2 shows spin-resolved ARPES spectra of the Shockley state of the Sb(111) surface, which is known as a typical case where the spin of the electron band is polarized along the plane due to the surface Rashba effect.[2] The spectra are recorded by four channeltrons in the Mott detector to measure the electron spin polarization of two orthogonal

directions, that is, in-plane and out-of plane to the (111) surface. As clearly seen, a pronounced peak at 0.1 eV in the up-spin spectrum of the in-plane direction is considerably reduced in the down-spin spectrum, in sharp contrast to the perfect superimposing of the up- and down-spin spectra of the out-of-plane direction. This result is in good agreement with the surface Rashba effect and unambiguously shows the spin-resolving performance of the developed photoemission system.



Fig. 1. Xenon-plasma discharge lamp

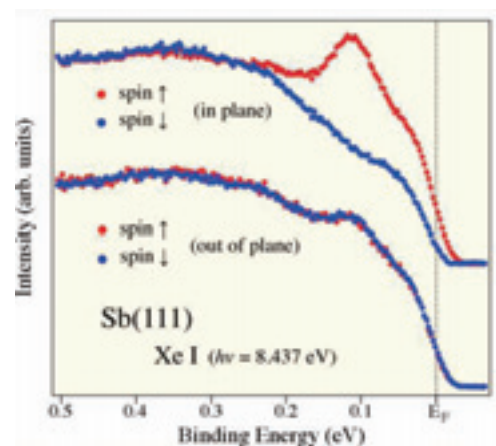


Fig. 2. Spin-resolved ARPES spectra of Sb(111)

[1] S. Souma *et al.*, RSI, **78** (2007) 123104.

[2] K. Sugawara *et al.*, PRL, **96** (2006) 046411.

Direct Domain Excitation by Photoemission and Its Dynamical Features Manifesting in ARPES spectra

K. Iwano

Photon Factory, Institute of Materials Structure Science, KEK, Tsukuba 305-0801, Japan

The theoretical and experimental studies of angle-resolved photoemission (ARPES) have focused on quasi-particle properties in various kinds of materials. Among them, heavily renormalized nature of quasi-particles typically seen in strongly-correlated electron systems have collected much attention, since the nature can provide important information on the many-body properties of those systems. However, even in such cases the quasi-particle basically consists of one hole; the strong renormalization only increases the particle mass and the lifetime. In this sense, what we observe in ARPES is inevitably of one-hole nature, however it is modified by interactions.

In this paper, we report on a completely different type of excitation that can be detected in the ARPES. In Fig. 1, we show a schematic picture in which a system that is located close to a phase boundary absorbed one high-energy photon. Assuming a valence photoemission, we are left with one hole in the valence band. In ordinary insulators, the process stops at this point. However, in this system, it does not stop but proceeds to form a domain [1]. We here think of a one-dimensional system whose ground state is expressed as in Fig. 1(a). TTF-CA, an organic molecular solid, is a system appropriate for this situation, having nearly degenerate neutral (N) and ionic (I) phases. In the process shown in Fig. 1(b), we expect that a domain of the I phase is created in the background of the N phase. It is emphasized that the driving force is the proximity to the N-I phase boundary combined with inherent electron itineracy, and that the detection of this process requires no pump-probe experiment but only an ordinary type of photoemission measurement.

In Fig. 2, we show calculated ARPES spectra (black lines) at two momenta, which are obtained very close to the phase boundary [2]. What is quite unique is that each spectrum exhibits a special spectral shape; the spectrum at $k=0$ takes a cusp-like shape, while the left-hand side of the spectrum at $k=\pi/2$ is almost fitted to a straight line. We also tried deriving an effective model that retains the two basic degrees of freedom of a single domain, namely, its center of gravity and its spatial size, plus spin degrees of freedom inside the domain. As a result of its analysis, we find that the effective model reproduces the spectral features, as shown by the red lines. In particular, the above-mentioned spectra shapes are

governed by the spin degrees of freedom, in a way that domain states with various spin configurations form a Hilbert space that can be accessed via the ARPES measurement.

This type of domain excitation is new in the ARPES studies, in the sense that it has never been observed so far. In addition to this, it also has important meaning in the context of photoinduced phase transitions. We hope for future experimental attempts that try to identify them in actual materials.

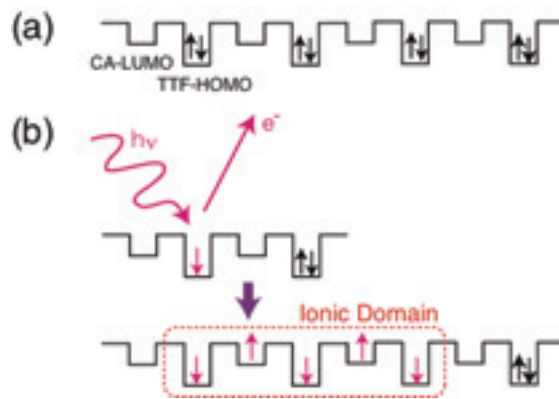


Fig. 1. (a) Neutral ground state and (b) schematic picture of an I-domain formation process.

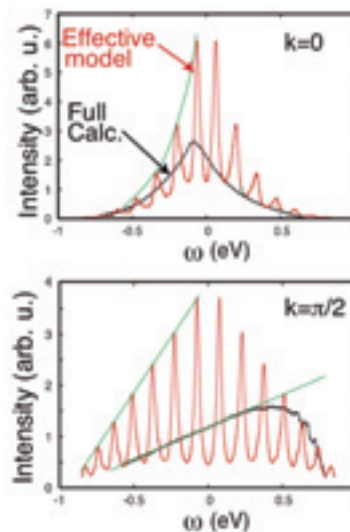


Fig. 2. Calculated ARPES spectra.

[1] K. Iwano, Phys. Rev. Lett., 97, 226404 (2006).
[2] K. Iwano, Phys. Rev. Lett. 102, 106405 (2009).

Valence-band Electronic Structure of FeSi studied by high-resolution Angle-Resolved Photoelectron Spectroscopy (ARPES)

Y. Takeichi¹, A. Nishide¹, K. Nakatsuji¹, T. Okuda¹, F. Komori¹, J. Yoshinobu¹, H. Kondoh², I. Matsuda¹, F. Bertran³, P. Le Fevre³, A. Taleb-Ibrahimi³, H. Yamagami⁴, A. Kakizaki¹

¹ISSP, the Univ. of Tokyo, Kashiwanoha, Kashiwa 277-8581, Japan

²Department of Chemistry, Keio University, Yokohama 223-8522, Japan

³SOLEIL / LURE, Saint-Aubin, BP 48, 91192 Gif-sur-Yvette Cedex, France

⁴Department of Physics, Kyoto Sangyo Univ., Kamigamo, Kita-ku, Kyoto 603-8555, Japan

Among transition metal mono-silicides: MSi (M=Cr, Mn, Fe, Co, Ni), FeSi has been intensively studied as one of the possible candidates for the d-electron Kondo insulators. While FeSi has an insulating ground state, electric conductivity shows a semiconductor to insulator crossover at 300K. Another interesting feature is the temperature dependence of its magnetic susceptibility, which rises nearly exponentially up to 500K making a broad maximum followed by a Curie-Weiss law at even high temperatures. To explain these unusual electric and magnetic properties, many theoretical models have been discussed so far. They are for example, thermally excited spin-fluctuation theory, phenomenological models assuming two narrow *d* bands in the vicinity of the band gap. Such a model density of states is quite similar to those for Kondo insulator description, and due to this similarity, it was often claimed that FeSi is the first Kondo insulator containing no *f*-electrons.

A number of valence band photoemission spectroscopy studies have been performed to elucidate the electronic structures near the Fermi level (E_F) [2]. In spite of careful measurement with sufficiently high-energy resolution smaller than the expected semiconductor band gap, results are not conclusive about the existence of the band gap [3]. Recently, Klein *et al.* made an effort to cleave a single crystal at (001) plane and observed ARPES spectra [4]. Though the sample surface consists of several faces, they observed that the spectral features are almost consistent with calculated band structure along the $\Gamma X\Gamma$ plane in the Brillouin zone showing a sharp peak feature at 300meV below E_F . In the following, we present the valence band structures of FeSi(001) single crystal surface observed by ARPES and discuss on the electronic structures of this material.

Experiments were carried out at CASSIOPEE beamline of SOLEIL. The ARPES apparatus consists of a sample preparation chamber equipped with an Auger electron spectrometer (AES) and a low energy electron diffraction (LEED) apparatus and an analysis chamber with a hemispherical electron energy analyzer (SCIENTA R4000). Clean FeSi(001) single crystal surface was obtained by the procedure described elsewhere [5].

Figure 1 shows the valence band structure of FeSi(001) single crystal surface observed along the Γ -X direction in the Brillouin zone, where the Fe *3d* originated valence band shows a very small energy dispersion. The results are basically consistent with the calculated valence band structure with an energy gap very close to the E_F . The obtained band dispersion well reproduces the theoretical calculation, except the reduction of the bandwidth of about 30% due to the renormalization effect.

This work resolves the controversial evidences, which have been provided for the arguments of the Kondo-like interaction in this material.

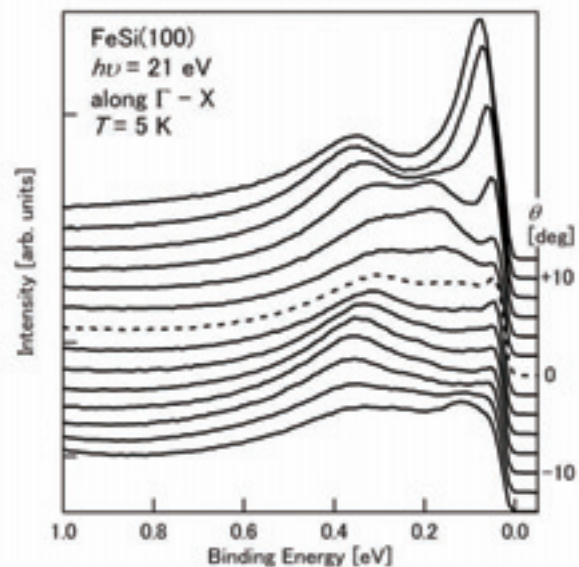


Fig. 1. ARPES spectra of FeSi(100).

- [1] C. Fu and S. Doniach, Phys. Rev. B **51**, 17439 (1995).
- [2] A. Kakizaki, *et al.*, J. Phys. Soc. Jpn., **51**, 2597 (1982).
- [3] K. Breuer, *et al.*, Phys. Rev. B **56**, R7061 (1995).
- [4] M. Klein, *et al.*, Phys. Rev. Lett., **101**, 046406 (2008).
- [5] K. Kura, *et al.* J. Phys. Soc. Jpn., **77**, 024709 (2008).

A topological metal at the surface of an ultrathin BiSb alloy film

T. Hirahara¹, Y. Sakamoto¹, Y. Saisyu¹, H. Miyazaki², S. Kimura²,
T. Okuda^{3,4}, I. Matsuda⁴, S. Murakami⁵, and S. Hasegawa¹

¹Department of Physics, University of Tokyo, 7-3-1 Hongo, Bunkyo-ku, Tokyo 113-0033, Japan

²UVSOR Facility, Institute for Molecular Science, Okazaki 444-8585, Japan

³Hiroshima Synchrotron Radiation Center, Hiroshima University,
Higashi-Hiroshima 739-0046, Japan

⁴Synchrotron Radiation Laboratory, ISSP University of Tokyo, Kashiwa 277-8581, Japan

⁵Department of Physics, Tokyo Institute of Technology, Tokyo 152-8551, Japan

Recently there has been growing interest in *topological insulators* or the *quantum spin Hall (QSH) phase*, which are insulating materials with bulk band gaps but have metallic edge states that are formed topologically and robust against any non-magnetic impurity [1]. In a three-dimensional material, the two-dimensional surface states correspond to the edge states (topological metal) and their intriguing nature in terms of electronic and spin structures have been experimentally observed in bulk $\text{Bi}_{1-x}\text{Sb}_x$ single crystals [2,3,4]. However, if we want to know the transport properties of these topological metals, high purity samples as well as very low temperature will be needed because of the contribution from bulk states or impurity effects. In a recent report, it was also shown that an intriguing coupling between the surface and bulk states will occur [5]. A simple solution to this bothersome problem is to prepare a topological metal on an ultrathin film, in which the surface-to-bulk ratio is drastically increased.

Therefore in the present study, we have investigated if there is a method to make an ultrathin $\text{Bi}_{1-x}\text{Sb}_x$ film on a semiconductor substrate. From reflection high-energy electron diffraction observation, it was found that single crystal $\text{Bi}_{1-x}\text{Sb}_x$ films ($0 < x < 0.25$) as thin as ~ 30 Å can be prepared on Si(111)-7x7. The transport properties of such films were characterized by *in situ* monolithic micro four-point probes [6]. The temperature dependence of the resistivity for the $x=0.1$ samples was insulating when the film thickness was 240 Å. However, it became metallic as the thickness was reduced down to 30 Å, indicating surface-state dominant electrical conduction. Figure 1 shows the Fermi surface of 40 Å thick $\text{Bi}_{0.92}\text{Sb}_{0.08}$ (a) and $\text{Bi}_{0.84}\text{Sb}_{0.16}$ (b) films mapped by angle-resolved photoemission spectroscopy. The basic features of the electronic structure of these surface states were shown to be the same as those found on bulk surfaces, meaning that topological metals can be prepared at the surface of an ultrathin film. The details will be given in the presentation.

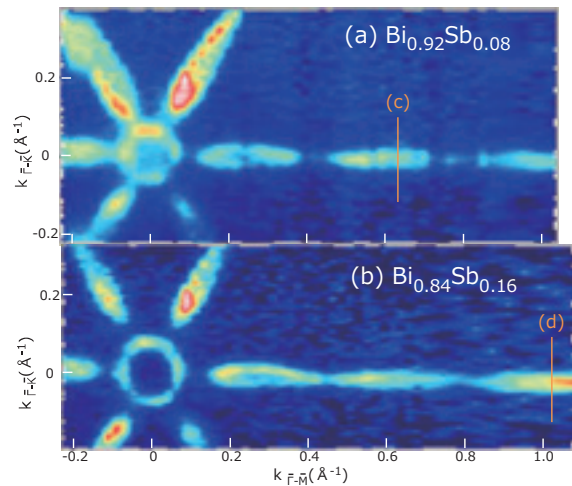


Fig. 1. The Fermi surface mapped by ARPES at 10 K for 40 Å thick $\text{Bi}_{0.92}\text{Sb}_{0.08}$ (a) and $\text{Bi}_{0.84}\text{Sb}_{0.16}$ (b) films, respectively. A circularly polarized light was used at the photon energy of 28 eV.

References:

- [1] L. Fu and C. L. Kane, Phys. Rev. B **76**, 045302 (2007).
- [2] D. Hsieh *et al.*, Nature **452**, 970 (2008).
- [3] D. Hsieh *et al.*, Science **323**, 919 (2009).
- [4] A. Nishide *et al.*, cond-mat/09022251, submitted to Phys. Rev. Lett. (2009)
- [5] A. A. Taskin and Y. Ando, Phys. Rev. B **80**, 085303 (2009).
- [6] T. Tanikawa *et al.*, e-Journal of Surface Science and Nanotechnology, **1**, 50 (2003).

Electronic Structure of Pseudo-one Dimensional $\text{Ba}_3\text{Co}_2\text{O}_6(\text{CO}_3)_{0.7}$

K. Soda¹, M. Kikuchi², S. Ogawa¹, H. Miyazaki^{1,3}, M. Inukai^{1,4}, M. Kato¹, S. Yagi¹,
K. Iwasaki^{1,5} and T. Matsui^{1,6},

¹Graduate School of Engineering, Nagoya University, Nagoya 464-8603 Japan

²School of Engineering, Nagoya University, Nagoya 464-8603 Japan

³UVSOR Facility, Institute for Molecular Science, Okazaki 444-8585, Japan

⁴Venture Business Laboratory, Nagoya University, Nagoya 464-8603 Japan

⁵Toyota Boshoku Coporation, Kariya 448-8651, Japan

⁶EcoTopia Science Institute, Nagoya University, Nagoya 464-8603 Japan

Cobalt oxides such as Na_xCoO_2 have attracted much attention because of their fascinating transport and magnetic properties. Recently it has been found that a barium cobalt oxycarbonate $\text{Ba}_3\text{Co}_2\text{O}_6(\text{CO}_3)_{0.7}$, which has pseudo-one dimensional structure with Co-O chains consisting of face-sharing CoO_6 octahedra along the c axis, shows a fairly large thermoelectric power factor of $0.9 \text{ mWm}^{-1}\text{K}^{-2}$ at 300 K with the thermoelectric power of about $+120 \mu\text{V K}^{-1}$ and metallic behavior of its electric conductivity above 300 K [1]. In this report, we have investigated its valence-band electronic structure by photoelectron spectroscopy to understand the physical properties.

Photoelectron measurements were carried out at the beamline BL-5U of UVSOR-II. Single crystalline specimens of $\text{Ba}_3\text{Co}_2\text{O}_6(\text{CO}_3)_{0.7}$ was prepared in size of $5 \times 0.5 \times 0.5 \text{ mm}^3$ by a flux method [1], and their clean surfaces was obtained by *in situ* fracturing the specimens in perpendicular to the c axis.

Figure 1 shows typical photoelectron spectra recorded at 20 K with the excitation photon energies $h\nu$ of 60 and 75 eV as well as their difference spectrum. Each spectrum is normalized with the integrated intensity and subtracted the background by an iteration method [2]. There are features A to H observed in the spectra; the features A to C are ascribed to the hybridized bands of the Co $3d$ and O $2p$ states, while the features D, F, G and H are assigned to the CO_3 -derived states, Ba $5p$ spin-orbit doublets and O $2s$ state, respectively. The feature E is attributed to the surface components. The remarkable suppression of the features A and B at $h\nu = 60 \text{ eV}$ is due to the Co $3p$ - $3d$ resonance, which indicates the relatively large Co $3d$ contribution to the features A and B while the O $2p$ one to the feature C.

Figure 2 shows detailed spectra near the Fermi level E_F measured at $h\nu = 40 \text{ eV}$ and several temperatures T in comparison with reference Au spectra. $\text{Ba}_3\text{Co}_2\text{O}_6(\text{CO}_3)_{0.7}$ reveals large reduction in intensity towards E_F but clear finite intensity at E_F . This may suggest the electron doping into the low-spin bands of $\text{Co}^{4+}(t_{2g}3d^5)$, which causes the positive thermoelectric power of 81 or $141 \mu\text{V K}^{-1}$ at high temperatures for the Co^{4+} concentration x of 0.7 [3], consistent with the observed value. Although a 1/8-power-law dependence of the intensity on the binding energy E_B

might be expected in one-dimensional fermion system [4], the anomalous exponents from 0.5 at 20 K to 0.8 at 200 K are obtained for $E_B = 0.01\text{--}0.1 \text{ eV}$, suggesting the larger short-range interaction at the lower temperature. A small hump at $E_B \sim 0.02 \text{ eV}$ observed at $T = 20 \text{ K}$ might also imply opening of a pseudogap or a magnetic ordering, which causes the recently observed reduction in the electric conductivity at low temperatures [5].

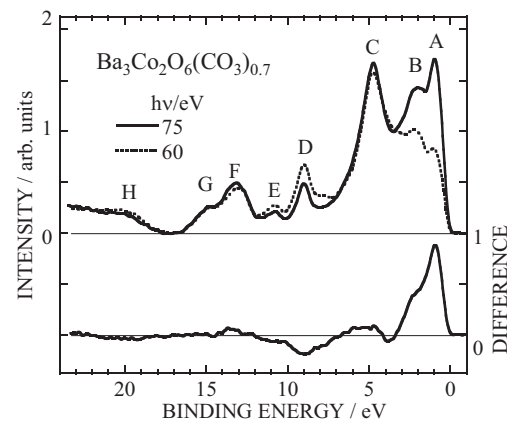


Fig.1. Valence-band spectra of $\text{Ba}_3\text{Co}_2\text{O}_6(\text{CO}_3)_{0.7}$.

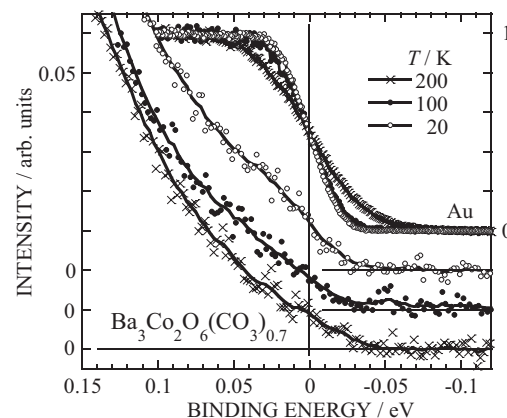


Fig.2. Valence-band spectra near the Fermi level.

- [1] T. Yamamoto *et al.*, Proc. Int. Symp. on EcoTopia Science 2007, p.145.
- [2] K. Soda *et al.*, J. Phys. Soc.Jpn. **60** (1991) 3059.
- [3] W. Koshibae *et al.*, Phys. Rev. B **62** (2000) 6869.
- [4] J. Voit, Pep. Prog. Phys. **57** (1994) 977.
- [5] K. Iwasaki, *private communication*.

Surface Chemistry of Butyl-Passivated Silicon Nanoparticles Studied by Synchrotron-Radiation Photoelectron Spectroscopy

M. Imamura, N. Takashima, J. Nakamura, S. Fujimasa, and H. Yasuda

Department of Mechanical Engineering, Kobe University, Kobe 657-8501, Japan

Various Si-based nanostructures have a great interest, since it has been reported that they show a strong photoluminescence, and therefore there is a possibility of future integrating electronic devices with optical sensing technique. Numerous works focused on the optical properties of Si nanoparticles prepared by various methods have been reported to date. However, data in the literatures are no universally accepted, and depend on various factors in the individual samples. Especially, the physical and chemical properties of nanoparticles are greatly influenced by surface chemical states due to the large surface to volume ratio with decreasing the size to the nanometer scale. In this work, we have synthesized n-butyl-passivated Si nanoparticles with well crystalline nature and well surface-passivated surface by the solution routes, and have directly characterized their electronic structures in the vicinity of Fermi level using synchrotron-radiation photo-electron spectroscopy. Furthermore, we have compared the valence-band photoemission spectra of fully n-butyl-passivated Si nanoparticles and those with oxygen contaminants in order to directly investigate the effect of surface chemical nature on their electronic structures.

Figure 1 shows the synchrotron-radiation valence-band photoemission spectra of as-prepared n-butyl-passivated Si nanoparticles with $d_c = 1.1$ nm and those exposed to ambient air for 10 min, on the HOPG substrate at room temperature with photon energy of 195 eV. The spectral features around 7 and 5.5 eV binding energies in the photoemission spectrum of as-prepared n-butyl-passivated Si nanoparticles originate from the C 2p derived states. The spectral feature around 7 eV binding energy originates from the C–H bonds in the butyl surface-passivants, and that around 5.5 eV binding energy originates from the Si–C bonds between the Si nanoparticle and butyl surface-passivants. This spectral feature around 5.5 eV in binding energy indicates that the present Si nanoparticles are well surface-passivated by butyl molecules. The spectral feature around 13.5 eV binding energy originates from the C 2s-derived states. The other spectral features around 3.5, 9, and 11 eV in binding energies originate from Si 3s- and 3p-derived electronic states. On the other hand, the valence-band photoemission spectrum of n-butyl-passivated Si nanoparticles with $d_c = 1.1$ nm after exposure to ambient air for 10 min is similar to that of as-prepared n-butyl-passivated Si nanoparticle. However, the spectral intensity derived from Si–C bonds around 5.5 eV binding energy

decreases with oxygen contaminants. This clearly indicates the removal of the surface-passivants of butyl molecules and subsequent contamination of oxygen. It should be noted that the valence-band photoemission spectrum of n-butyl-passivated Si nanoparticles with oxygen contaminants exhibits an additional feature centered around 2.6 eV binding energy (shown by the arrow). Puzder *et al.* have previously reported the Density of State (DOS) of hydrogen-passivated Si nanoparticles with various contaminants by means of local density approximation (LDA) in order to see physical origin of the effect of oxygen on the gap. [1] When a double bonded contaminant such as oxygen and sulfur is added to Si nanoparticles, the Si sp_3 network is considerably distorted and the HOMO and LUMO change their nature significantly. As a result, HOMO and LUMO states localized in the vicinity of the Si=O double bond, and the modified DOS originated from the HOMO and LUMO appears near the Fermi level as the additional features. From the comparison with this LDA theoretical DOS, it is concluded that this additional feature is ascribed to oxygen-contaminants-induced states, and this result provides a direct evidence of the effect of oxygen contaminants on the electronic structure that the previous calculation has predicted.

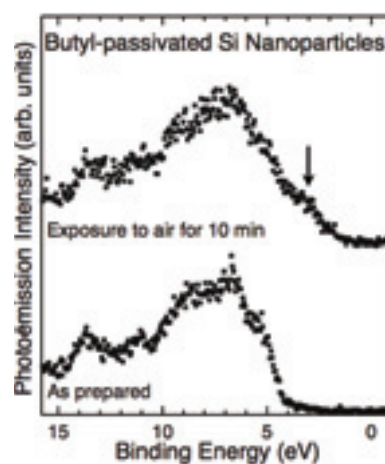


Figure. 1 Valence-band photoemission spectrum of as-synthesized n-butyl-passivated Si nanoparticles with $d_c = 1.1$ nm and those exposed to air for 10 min. The arrow indicates the additional feature originated from the oxygen-contaminant-induced states.

[1] A. Puzder, A. J. Williamson, J. C. Grossman, and G. Galli, *Phys. Rev. Lett.*, **88**, 097401 (2002).

Low-energy angle-resolved photoemission spectroscopy of Fe-based high- T_c superconductor $\text{Ba}_{1-x}\text{K}_x\text{Fe}_2\text{As}_2$

K. Nakayama¹, K. Terashima², T. Sato^{1,3}, T. Kawahara¹, Y. Sekiba¹, T. Qian¹, P. Richard⁴, S. Souma⁴, T. Ito², S. Kimura², G. F. Chen⁵, J. L. Luo⁵, N. L. Wang⁵, H. Ding⁵ and T. Takahashi^{1,4}

¹*Department of Physics, Tohoku University, Sendai 980-8578, Japan*

²*UVSOR Facility, Institute for Molecular Science, Okazaki 444-8585, Japan*

³*TRiP, Japan Science and Technology Agency (JST), Kawaguchi 332-0012, Japan*

⁴*WPI Research Center, Advanced Institute for Materials Research, Tohoku University, Sendai 980-8577, Japan*

⁵*Beijing National Laboratory for Condensed Matter Physics, and Institute of Physics, Chinese Academy of Sciences, Beijing 100190, China*

The recent discovery of high- T_c superconductivity in iron pnictide compounds has generated fierce debates on the high- T_c mechanism. The parent compounds of iron pnictide superconductors exhibit long-range antiferromagnetic order below T_N accompanied by the structural phase transition. By doping hole or electron carriers, the magnetic and structural phase transitions are suppressed and eventually the superconductivity emerges. To clarify the superconducting mechanism, it is essentially important to understand the doping-induced evolution of the low-energy band structures responsible for the emergence of the superconductivity. The understanding of the superconducting gap character is also critically important, since it is intimately related to the superconducting pairing interactions. To elucidate these points, we have performed high-resolution angle-resolved photoemission spectroscopy (ARPES) on $\text{Ba}_{1-x}\text{K}_x\text{Fe}_2\text{As}_2$.

ARPES measurements were performed using MB Scientific A1 spectrometer at the beamline 7U of UVSOL-II. We used low-energy photons ($h\nu = 6\text{-}25$ eV) to excite photoelectrons. The energy resolution was set to 8-14 meV.

Figure 1 (a) shows the ARPES spectral intensity of optimally hole-doped $\text{Ba}_{0.6}\text{K}_{0.4}\text{Fe}_2\text{As}_2$ ($T_c = 37$ K) measured at 17 K along the red line in the Brillouin zone shown in the inset. We clearly observed a hole-like band centered at the Γ point. In Fig. 1(b), we show the ARPES spectrum measured at the Fermi wave vector of this band. A sharp quasiparticle peak together with a leading-edge shift toward higher binding energy is clearly seen, indicating a superconducting gap opening. The superconducting gap size (Δ) estimated from the peak position is about 10 meV. This is significantly larger than the value (~ 5.5 meV) expected from the weak-coupling theory, suggesting an anomalously strong-coupling nature of the superconductivity in this compound. In this presentation, we also discuss the doping dependence of the electronic structures in relation to the occurrence of the superconductivity.

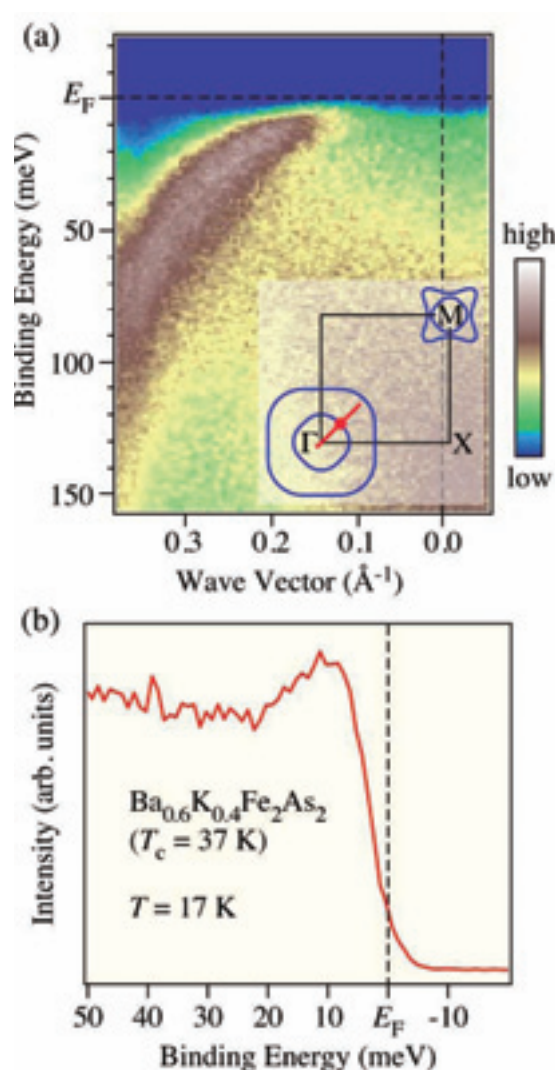


Fig. 1. (a) ARPES intensity plot near the Γ point of $\text{Ba}_{0.6}\text{K}_{0.4}\text{Fe}_2\text{As}_2$ ($T_c = 37$ K) as a function of binding energy and wave vector measured at 17 K with 21 eV photons. The inset indicates schematic Fermi surfaces (blue curves) and the measurement location (red line). (b) High-resolution ARPES spectrum near E_F at 17 K measured at the Fermi vector of the hole-like band (red circle).

Magnetic Circular Dichroism in Valence Band using Laser Excitation

T. Nakagawa, I. Yamamoto, Y. Takagi and T. Yokoyama

Department of Electronic Structure, Institute for Molecular Science, Okazaki 444-8585, Japan

Recently the magnetic circular dichroism has been a widely used method since it can detect the magnetic properties of thin films without spin detector, namely the measurement is simple and efficient. However valence band magnetic circular dichroism is generally known to be tiny due to the weak spin orbit coupling in valence band. Together with angle and energy resolved photoemission, it has been revealed that the MCD asymmetry is large enough to be measured ($\sim 10\%$). [1] Enhanced MCD also can be obtained in threshold photoemission with total electron yield method, [2,3] but away from the threshold the MCD asymmetry is drastically reduced. Since the valence band electron excitation is achieved by pulse lasers, it is expected that MCD in valence band would be investigated by multiphoton process. [4] Although in principal the multiphoton MCD process is possible, it is completely unclear how much asymmetry is achieved.

We report an observation of two photon photoemission (2PPE) magnetic circular dichroism (MCD) on Ni(15 ML)/Cu(001) near the Fermi level using short pulse laser. [1, 2] Figures 1(a) and (b) show ARPES spectra and the MCD asymmetry for 2PPE. The spectra are taken along the surface normal using circularly polarized light. Ni 3d peak are observed near the Fermi level, and the 3d peak shows slight shift by inverting the direction of the magnetization, which is the manifestation of MCD. The derived MCD spectra show $\sim 20\%$ asymmetry

The reduction of Ni MCD asymmetry by the overlayer metal capping is examined. It is believed that the electron escape depth for low kinetic energy is large, ~ 10 nm. However the estimation of the escape depth usually neglects the diffraction effect of electrons by overlayers, which is significantly important for the angle resolved photoemission experiments. Fig.1 (c) plots the variation of the MCD asymmetry by increasing the Cu overlayer onto the Ni film and it is found that for the electron kinetic energy of ~ 1 eV the attenuation depth is only ~ 2 ML (0.32 nm) for Cu deposition, which is much smaller than the escape depth by universal curves (~ 10 nm). This reduced electron escape depth is explained by electron diffraction effects when the photoelectrons pass through the capping layer.

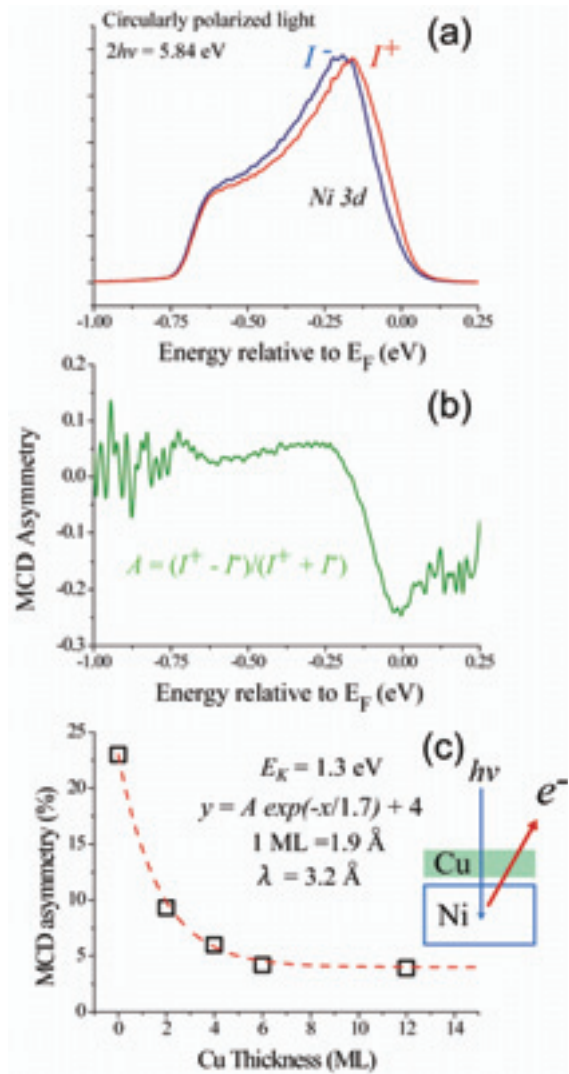


Fig. 1 (a) Two photon ARPES spectra for Ni(15 ML)/Cu(001) sample. The sample magnetization is inverted by pulse coil and the helicity of the circularly polarization is fixed. (b) MCD asymmetry derived from the spectra in (a). (c) The variation of the MCD asymmetry by increasing the thickness of Cu overlayer.

[1] T. Nakagawa, and T. Yokoyama, *Phys. Rev. Lett.* **96**, 237402(2006).

[2] T. Nakagawa *et al.*, *Phys. Rev. B.* **79**, 172404 (2009).

In situ photoelectron spectra of an electron-beam irradiated C₆₀ film

J. Onoe^{1*}, T. Ito², S. Kimura³, H. Shima⁴ and H. Yoshioka⁵

¹Research Laboratory for Nuclear Reactors and Department of Nuclear Engineering, Tokyo Institute of Technology, Tokyo 152-8550, Japan

²Department of Materials, Physics and Energy Engineering, Nagoya University, Nagoya 464-8601, Japan

³UVSOR Facility, Institute for Molecular Science, and School of Physical Sciences, The Graduate University for Advanced Studies (SOKENDAI), Okazaki 444-8585, Japan

⁴Department of Applied Physics, Hokkaido University, Sapporo 060-8628, Japan

⁵Department of Physics, Nara Women's University, Nara 630-8506, Japan

We have found that electron-beam (EB) irradiation of a C₆₀ film gives rise to formation of a peanut-shaped C₆₀ polymer with metallic electron-transport properties in air at room temperature [1]. The temperature dependence of the photo-excited carriers lifetime for the peanut-shaped polymer indicated the energy gap formation at below 50 K in a similar manner to the Peierls instability for quasi-one-dimensional (1D) metallic materials such as K_{0.3}MO₃ [2], thus suggesting that the polymer is a 1D metal as illustrated in Fig. 1.

The 1D peanut-shaped polymer is fascinating from a viewpoint of topology, because it has both positive and negative Gaussian curvatures (κ) lined alternatively and periodically. As shown in Table 1, this nanocarbon can be classified into a new π -electron conjugated carbon allotrope that is different from graphite ($\kappa = 0$), fullerenes ($\kappa > 0$), nanotubes ($\kappa = 0$ at body, $\kappa > 0$ at cap edge), and hypothetical Mackay crystal ($\kappa < 0$). Accordingly, the 1D peanut-shaped polymer is expected to exhibit physical and chemical properties different from those of the conventional π -electron conjugated carbon materials.

We have recently examined the valence photoelectron spectra of the polymer, using *in situ* high-resolution ultraviolet photoelectron spectroscopy [3, 4], and observed the Tomonaga-Luttinger liquids (TLL) behavior as the direct evidence for 1D metal and obtained the TLL exponent (α) to be ca. 0.6 [5], which is somewhat larger than that of ca. 0.5 for 1D metallic single-walled carbon nanotubes [6]. Using the Schrodinger equation dealing with the motion of free particles on a curved surface modulated by positive and negative Gaussian curvatures periodically and alternatively, we have first demonstrated that the increase in the exponent value is caused by a curvature-induced effective potential that works for electrons conducting along the curved surface [7].

To our best knowledge, the peanut-shaped C₆₀ polymer is only an existed material with a negative Gaussian curvature, whose electronic and optical properties are revealed. Thus we believe that the present system will open a new field of “quantum

science of condensed matters in Liemannian space”.

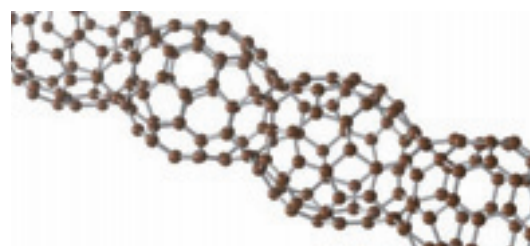


Fig. 1. Schematic illustration of one-dimensional peanut-shaped C₆₀ polymer.

Table 1. Classification of π -electron conjugated carbon materials using Gaussian curvature.

Material	Gaussian curvature (K)
Graphite	0
Fullerenes	> 0
Nanotubes	0 (body), > 0 (capped edge)
Mackay crystal	< 0
Peanut-shaped polymer	> 0, < 0

*E-mail: jonoe@nr.titech.ac.jp

[1] J. Onoe, T. Nakayama, M Aono, and T. Hara, Appl. Phys. Letters **82** (2003) 595.

[2] Y. Toda, S. Ryuzaki, and J. Onoe, Appl. Phys. Letters **92** (2008) 094102.

[3] J. Onoe *et al.*, Phys. Rev. B **75** (2007) 233410.

[4] J. Onoe, T. Ito, and S. Kimura, J. Appl. Phys. **104** (2008) 103706.

[5] T. Ito, J. Onoe, H. Shima, H. Yoshioka, and S. Kimura, in preparation for submission.

[6] H. Ishii *et al.*, Nature **426** (2003) 540.

[7] H. Shima, H. Yoshioka, and J. Onoe, Phys. Rev. B **79** (2009) 201401 (R).

Electronic structure of $\text{Mn}_3\text{Cu}_{1-x}\text{Ga}_x\text{N}$ studied by soft X-ray photoelectron spectroscopy

Y. Miyata¹, K. Mima¹, R. Yamaguchi¹, A. Yamasaki², A. Higashiya³, T. Muro⁴,
K. Terashima¹, K. Takenaka⁵, A. Ozawa⁵, T. Inagaki⁵, S. Imada¹

¹ Department of Physics, Ritsumeikan University, Kusatsu, Shiga 525-8577, Japan.

² Department of Physics, Faculty of Science and Engineering, Konan University, Kobe
658-8501, Japan

³ SPring-8 / RIKEN, Hyogo 679-5148, Japan

⁴ JASRI, SPring-8, Hyogo 679-5198, Japan

⁵ Department of Crystalline Materials Science, Nagoya University, Nagoya 464-8603, Japan

Antiperovskite manganese nitrides Mn_3XN (A=Zn, Ga, etc) are potential candidates for large negative thermal expansion (NTE) materials. These nitrides are well known for their large magnetovolume effect (MVE) [1]. Unlike other Mn_3XN , Mn_3CuN does not show MVE. Instead, Mn_3CuN undergoes a first-order transition from the high-temperature paramagnetic to the low-temperature ferromagnetic phase at $T_C=143\text{K}$, accompanied by cubic-to-tetragonal structural deformation [2].

In order to clarify the relationship between crystal structure and magnetic structure in this system, we studied the electronic states of $\text{Mn}_3\text{Cu}_{1-x}\text{Ga}_x\text{N}$ by soft X-ray photoelectron spectroscopy (SXPES). We have also carried out band structure calculation, and compared the obtained electronic structures with the experimental results. Figure 1 shows the valence band SXPES spectra of Mn_3CuN and $\text{Mn}_3\text{Cu}_{0.5}\text{Ga}_{0.5}\text{N}$, the latter showing MVE, measured with the incident photon energy of 700 eV. Both spectra consists of three characteristic structures; a peak in the vicinity of Fermi level, a peak at 3.5 eV, and a hump at ~ 8 eV. From the comparison between the SXPES result and band calculation, we identify each as mainly N 2p, Cu 3d, and Mn 3d bands, respectively. Next we compared the electronic states of $\text{Mn}_3\text{Cu}_{0.5}\text{Ga}_{0.5}\text{N}$ with Mn_3CuN . Through the substitution of Ga for Cu, the photoelectron intensity peak at 3.5 eV decreases, whereas the peak in the vicinity of Fermi level becomes sharper. These changes are consistent with the results of the band calculation.

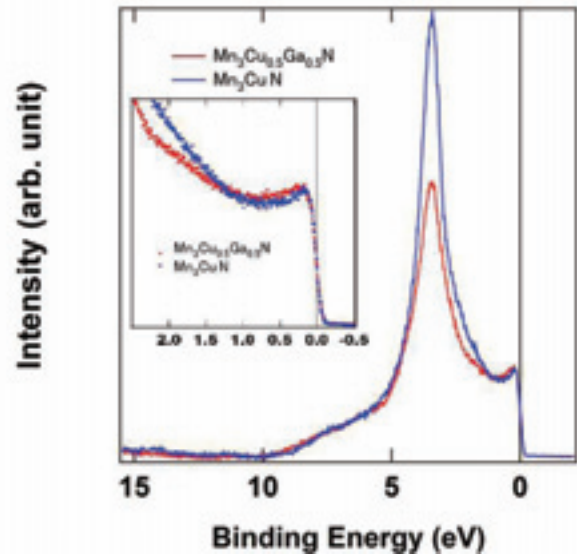


Fig. 1. SXPES spectra of Mn_3CuN and $\text{Mn}_3\text{Cu}_{0.5}\text{Ga}_{0.5}\text{N}$. In the main panel, the lines represent the spectra measured at 170K (paramagnetic phase), respectively. These spectra are normalized by the integrated intensity. The inset shows the magnified view of the spectra near the Fermi level where the red filled circles and the blue filled circles represent the spectra in Mn_3CuN and $\text{Mn}_3\text{Cu}_{0.5}\text{Ga}_{0.5}\text{N}$ respectively.

[1] K. Takenaka *et al.*, Appl. Phys. Lett. **87** 261902 (2008)

[2] K. Takenaka *et al.*, Appl. Phys. Lett. **92** 161909 (2008)

“L+1 rule” for continuous electron-hole excitations in photoemission spectra

V. I. Grebennikov, T.V. Kuznetsova.

Institute of Metal Physics, UD RAS, Ekaterinburg 620041, Russia

Low-energy excitations in valence bands are studied by means of XPS spectroscopy. The analysis of a form of core levels spectra gives the size of effects of electron-hole interactions on atoms of different chemical elements in the compound $\text{Ni}_{0.5}\text{TiTe}_2$. The rule for many-electron excitations in solids under action of core-level photo holes is offered.

$\text{Ti}2p$ and $\text{Te}3d$ XPS spectra in the intercalated compound $\text{Ni}_{0.5}\text{TiTe}_2$ are shown in fig. 1. The lines of the $\text{Ti}2p$ spin-orbital doublet are broadened asymmetrically due to many-body excitations of valence-band electrons generated by sudden creation of the $2p$ photo holes [1]. At the same time such effects on the $\text{Te}3d$ lines are much smaller. To extract the quantitative information the experimental spectra were approximated by a sum of two spin-orbital lines and an inelastic background I_{bg} : $I(E) = I_1(E) + I_2(E) + I_{bg}(E)$. The form of each line $I_j(E) = A_j \text{Im}g(E - E_j - i\Gamma_j)$ is determined by an imaginary part of the power function [2]

$$g(z) = \frac{1}{(1-\alpha)b} [1 - (1 - b/z)^{1-\alpha}] \quad (1)$$

Here A_j is line weights; α is the asymmetry coefficient, shown intensity of the valence electron excitations accompanying creation of the photo hole; b is their maximal energy; E_j and Γ_j stand for binding energy and decay of the lines. The power of electron-hole interaction for different XPS lines in $\text{Ni}_{0.5}\text{TiTe}_2$ has the following magnitudes:

Line	Ti2p	Te3d	Ti 3s	Te4d
α	0.33	0.06	0.23	0.08

The asymmetry of a spectrum (dynamic screening of the photo hole) in titanium is much more, than in other components of compound. It is characterized by $\alpha = 0.33$ (the values of α in nickel and tellurium are small, see table and spectra). The important conclusion follows. Despite of a collective character of the valence band electrons in solids, their reactions on photo holes, arising on core levels of various elements, are completely different. Exaggerating, it is possible to tell, that in this case there is no common band excitations, each atom in itself.

Analyses of XPS spectra of $\text{Ni}_{0.5}\text{TiTe}_2$ and other compounds allow us to conclude that the many-body excitations in solids are followed by the “ $l + 1$ rule”: photo-hole with the moment l shakes up the band electrons of $l + 1$ states, mainly. So, for example, $3d$ -electrons react basically on $2p$ -hole, therefore the many-electron effects are strongest on titanium atoms.

These effects are smaller on nickel atoms because of the almost filled Ni $3d$ -shell does not respond on external perturbations. The Te $3d$ - and $4d$ -spectra are narrow symmetric lines like in an isolated atom because of f -electrons absence.

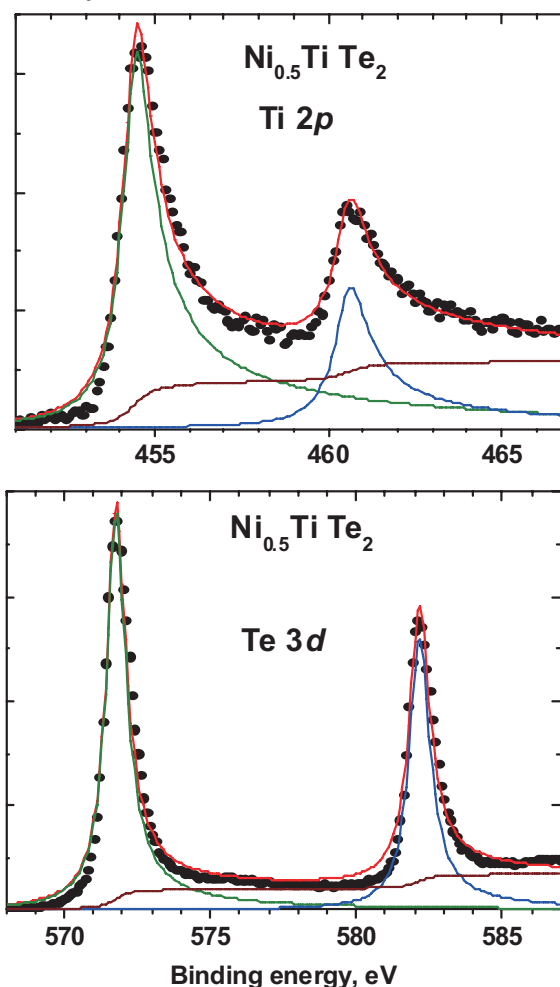


Fig. 1. $\text{Ti}2p$ and $\text{Te}3d$ XPS spectra in the compound $\text{Ni}_{0.5}\text{TiTe}_2$ and their decomposition on sum of two standard lines (1) and a background.

The origin of the rule is connected to prevalence of the dipole matrix elements in coulomb interaction $l' = l \pm 1$. However the probability of a transition with reduction of the orbital moment in solids is much less than that in free atoms because of strong delocalization of electron states with the moment $l - 1$. In result the $l + 1$ transition dominate, as it is clearly visible in experimental spectra.

[1] S. Doniach, M. Sundjic, J. Phys. C **3** (1970) 285.

[2] V. I. Grebennikov, J. Electr. Spectr. Rel. Phenom. **137-140** (2004) 741.

Temperature and substitution dependence of extremely low-energy photoemission spectra on $\text{Sm}_{1-x}\text{Eu}_x\text{B}_6$

J. Yamaguchi¹, A. Sekiyama¹, M. Y. Kimura¹, H. Sugiyama¹, S. Komori¹, Y. Tomida¹, G. Kuwahara,¹ T. Ito², S. Kimura², S. Yeo³, S.-I. Lee⁴, H.-D. Kim⁵, and S. Suga¹

¹Graduate school of Engineering Science, Osaka University, Toyonaka, Osaka 560-8531, Japan

²UVSOR Facility, Institute for Molecular Science, Okazaki 444-8585, Japan

³Korea Atomic Energy Research Institute, Daejeon 305-6000, Korea

⁴Department of Physics, Sogang University, Seoul 121-742, Korea

⁵Pohang Accelerator Laboratory, Pohang 790-784, Korea

SmB_6 and YbB_{12} have been well known as valence fluctuating (VF) Kondo semiconductors (insulators) and intensively studied because of their physical properties. The Kondo semiconductors behave as metals with localized f magnetic moments at high temperatures (T), whereas they develop a narrow hybridization gap (~ 10 meV) at the Fermi level (E_F) at low T . It is thought that the gap formation originates from the hybridization of the narrow f band with broad itinerant valence-bands, but the mechanism of the gap is still controversial.

In our previous hard x-ray photoemission (HAXPES) studies for the Lu substitution Kondo semiconductor alloys $\text{Yb}_{1-x}\text{Lu}_x\text{B}_{12}$ [1], we have found from the T dependence of the Yb $4f$ spectral analyses that the $4f$ lattice coherence plays important roles for developing the gap. The gap for YbB_{12} is suggested to be rapidly closed by the Lu substitution of $x = 0.125$ due to the collapse of the $4f$ lattice coherence. On the other hand, our HAXPES study for the Eu substitution alloys $\text{Sm}_{1-x}\text{Eu}_x\text{B}_6$ shows that the T dependence of the Sm^{2+} $4f$ spectra for $x = 0.15$ is qualitatively similar to that for pure YbB_{12} . Thus, it is expected from our HAXPES results that a finite gap is still open for $\text{Sm}_{0.85}\text{Eu}_{0.15}\text{B}_6$, although the $4f$ lattice coherence could be broken by the Eu substitution. In order to directly investigate the existence of the gap, we have performed the extremely low-energy photoemission (ELEPES) study on $\text{Sm}_{1-x}\text{Eu}_x\text{B}_6$ ($x = 0, 0.15,$ and 0.5). The ELEPES spectra for $x = 0.15$ and 0.5 were measured by use of synchrotron radiation ($h\nu = 7$ eV) at UVSOR-II BL7U and those for $x = 0$ and 0.5 were measured with the Xe I ($h\nu = 8.4$ eV) resonance line. The energy resolution was set to ~ 6 meV in all measurements.

Figure 1 shows the T dependence of the ELEPES spectra near E_F for $x = 0, 0.15,$ and 0.5 . According to the photoionization cross section [2], the observed spectra are dominated by the non- $4f$ (Sm and/or Eu $5d$ and B $2sp$) states. For $x = 0$, we find that a so-called leading-edge of the spectra is on the occupied side, which indicates the existence of the finite gap. In addition, the prominent peak is observed at ~ 15 meV, which is comparable to that due to the magnetic excitation observed by neutron scattering

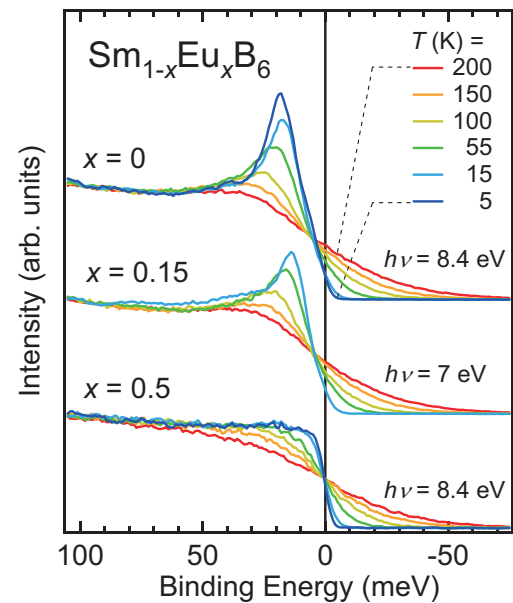


Fig. 1. Temperature dependence of the ELEPES spectra near E_F for $\text{Sm}_{1-x}\text{Eu}_x\text{B}_6$.

measurements for SmB_6 [3]. With increasing T from 5 to 200 K, the spectral weight on E_F increases and the peak shifts toward the higher binding energy side. It should be noted that the spectra for $x = 0.15$ show the essentially equivalent T dependence for $x = 0$, which indicates that $\text{Sm}_{0.85}\text{Eu}_{0.15}\text{B}_6$ is still a Kondo semiconductor against the collapse of the $4f$ lattice coherence. In contrast, the spectra for $x = 0.5$ show no prominent peak and thus a typical metallic thermal behavior. These ELEPES results indicate that SmB_6 is a “robust” Kondo semiconductor against a rare-earth substitution, which is significantly different from YbB_{12} .

[1] J. Yamaguchi *et al.*, Phys. Rev. B **79**, 125121 (2009).

[2] J. J. Yeh and I. Lindau, At. Data Nucl. Data Tables **32**, 1 (1985).

[3] P. A. Alekseev *et al.*, J. Solid State Chem. **133**, 230-236 (1995).

SOLEIL, Cassiopée

ARPES and spin resolved Investigations on the 8-1500 eV high resolution Cassiopée beamline at SOLEIL

Alessandro Nicolaou^{1,2}, François Bertran, Patrick Lefevre¹, Antonio Tejada¹, Julien Pinon, Daniel Ragonnet and Amina Taleb-Ibrahimi*

¹*Synchrotron SOLEIL, GIF-sur-YVETTE, France*

²*Lab. Physique des Solides, Université Paris-Sud XI, Orsay, France*

In this poster an overview of the performances of the high resolution Photoemission Beamline Cassiopée at SOLEIL will be shown.

This beamline is divided in two branches dedicated to High energy resolution ARPES and spin –resolved photoemission.

We will present an angle-resolved photoemission (ARPES) study of the low energy electronic structure of “misfit” cobaltates. Misfits are lamellar compounds, where metallic CoO₂ layers are separated by an “insulating” rock-salt structure, which acts as charge reservoir. The two sub-structures are generally incommensurate, this is why they are called misfit. In 2003, Takada et al. observed superconductivity along the same CoO₂ in Na_{0.3}CoO₂:2H₂O . Since then, the family of Na_xCoO₂, are heavily studied and showed a rich phase diagram in function of electron doping, from the Mott insulator limit (CoO₂) to the band insulator NaCoO₂ . The “misfits” are located near the band insulator limit (X=0.7-1) and show coexistence of high thermoelectric power, good metallicity and Curie-Weiss susceptibility as Na cobaltates of the same doping. However, the transport properties suggest an evolution toward an insulating phase before the band insulator limit, not observed in Na cobaltates. We are interested in the comparison between the two systems to understand what is intrinsic of the metallic CoO₂ layers.

In addition, spin polarized photoemission data on Cassiopée allowing the determination of the polarization at the Fermi level in epitaxial FeV alloys, a step toward the understanding of the tunnel transport in MgO epitaxial junctions using these alloys as electrodes, will be shown.

* amina.taleb@synchrotron-soleil.fr

Temperature Dependent Angle-Resolved Photoemission Spectroscopy on Ferromagnetic EuO Thin Films

H. Miyazaki¹, T. Ito², H. J. Im³, S. Yagi², M. Kato², K. Soda² and S. Kimura^{1,4}

¹UVSOR Facility, Institute for Molecular Science, Okazaki 444-8585, Japan

²Graduate School of Engineering, Nagoya University, Nagoya 464-8603, Japan

Department of Advanced Physics, Hirosaki University, Hirosaki 036-8560, Japan

⁴School of Physical Sciences, The Graduate University for Advanced Studies, Okazaki 444-8585, Japan

Europium monoxide (EuO) is a ferromagnetic semiconductor with the Curie temperature (T_C) at around 70 K [1, 2]. In the electron doping case by the Eu excess or substitute Gd^{3+} or La^{3+} from Eu^{2+} ion, the T_C increases up to 150 K and the electrical resistivity drops twelve-order of magnitude below the T_C originating in a metal-insulator transition (MIT) [2, 3]. To reveal the origin of these physical properties of EuO, it is important to clarify the electronic structure. Three dimensional angle-resolved photoemission spectroscopy (3D-ARPES) using a synchrotron radiation source is the most powerful technique to directly determine the electronic band structure. Using this technique we observed the change in the Eu 4f and O 2p states across T_C .

Single-crystalline EuO thin films with a thickness of about 50 nm were fabricated by the molecular beam epitaxy (MBE) [4]. Epitaxial growth of the single-crystalline EuO thin films with the 1 x 1 EuO (100) patterns was confirmed with low energy electron diffraction (LEED) and reflection high energy electron diffraction (RHEED) methods. The T_C measured with a superconducting quantum interference device (SQUID) magnetometer was 71 K. The 3D-ARPES measurements were performed at the beam line 5U of UVSOR-II combined with the MBE system.

Figures 1(g1) [1(g2)] and 1(x1) [1(x2)] show the temperature dependence of the Eu 4f [O 2p] band at the Γ and X points, respectively. The circles and bright area correspond to the peak positions of the second-derivative energy distribution curves (EDCs). With decreasing temperature across T_C , all of the bands shift by 0.2–0.3 eV to the lower binding energy side. The overall energy shift is in good agreement with the magnetic red shift estimated from the optical absorption spectra [5]. This indicates that the overall energy shift originates from the changing of the bottom energy of the Eu 5d conduction band at the X point due to the energy gain of the Eu 5d majority-spin state after band splitting caused by ferromagnetic ordering. In addition, the top of the Eu 4f states is shifted away from the main 4f states at the Γ and X points. In contrast, the O 2p state is splitted into two bands below T_C . The bands at the higher and lower binding energies are attributed to the majority and minority spin states, respectively. Since the Eu 4f state is fully polarized, the 4f state mainly hybridizes

with the majority spin state of O 2p and Eu 5d. Therefore, the band shifts can be attributed to the hybridization effect between the Eu 4f and O 2p states (superexchange interaction) and between the Eu 4f and 5d states (indirect exchange interaction). The observed temperature dependent energy shift of the 4f state is the essential origin of the ferromagnetic phase transition of EuO.

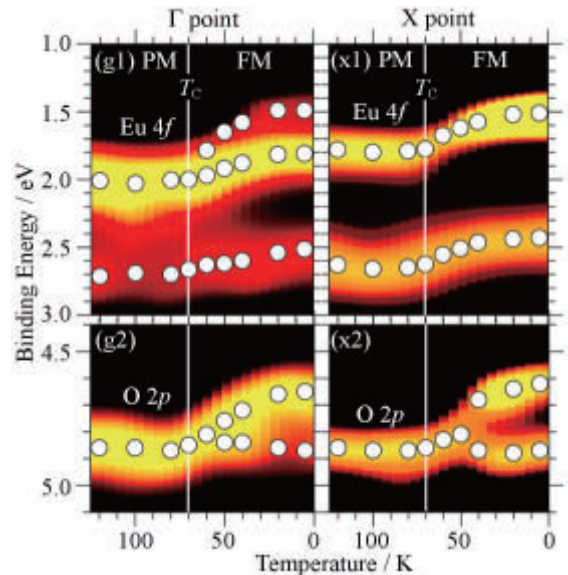


Fig. 1 Temperature dependence of the photoemission peak energies derived from the second-derivative EDCs of the Eu 4f [(g1), (x1)] and O 2p [(g2), (x2)] states at the Γ and X points. The open circles indicate the peaks of the second derivative EDCs.

- [1] N. Tsuda *et al.*, *Electronic Conduction in Oxides* (Springers College) (1976).
- [2] A. Mauger *et al.*, *J. Phys. (paris)* **39**, 1125 (1978).
- [3] Y. Shapira, S. Foner, and T. B. Reed, *Phys. Rev. B* **8**, 2299(1973); **8**, 2316 (1973).
- [4] H. Miyazaki *et al.*, *Jpn. J. Appl. Phys.* **48**, 055504 (2009).
- [5] S. Kimura *et al.*, *Phys. Rev. B* **78**, 052409 (2008).

Present status of VUV angle-resolved photoemission beamline BL7U at UVSOR-II

T. Ito^{1,2}, M. Sakai¹, E. Nakamura¹, N. Kondo¹, and S. Kimura^{1,2}

¹UVSOR Facility, Institute for Molecular Science, Okazaki 444-8585, Japan

²School of Physical Sciences, the Graduate University for Advanced Studies (SOKENDAI), Okazaki 444-8585, Japan

BL7U, the VUV angle-resolved photoemission (ARPES) beamline for advanced studies of strongly correlated electron systems, has been constructed in FY2006 and opened for users in FY2007 [1]. To satisfy the needs from users, especially (1) higher photon-flux, (2) reduction of higher-order light and (3) better base pressure of the photoemission chamber, we have improved the beamline in FY2008. As a result, we successfully achieved the sufficient throughput for ARPES experiments.

To improve the photon-flux especially at the bulk-sensitive low photon-energy ($h\nu < 15$ eV), we updated the lowest photon-energy grating G3 from Au-coating to SiC-coating one. After the update of G3, we realign the beamline to be optimized with the center of the undulator light. As a result, the photon flux as well as the focusing at the sample position has intensively been improved than that in FY2007. Figures 1(a), (b) and (c) show the improved throughput spectra obtained at low (red line)-, medium (red line)-, and high (red, yellow, green, blue lines)-photon energy regions compared with the previous one (black lines), respectively. At each energy region, the spectrum becomes sharper and shifts to the higher energy side in the same condition, indicating successful alignment with the optimum parameter of the undulator light. Clear vibration sub-bands observed higher and lower energy side of the main peak of the throughput spectrum (Fig. 2), which is consistent with a calculation, ensures the correct alignment getting the center of the undulator light.

To reduce the intensity of higher order light at the low photon-energy region, we equipped a VUV filter of MgF_2 just after the exit slit. As a result, we successfully reduced the higher-order light above $h\nu = 11$ eV (see Fig. 3). Typical loss of efficiency by the filter is less than 10%, which ensures sufficient throughput for VUV ARPES experiments with bulk-sensitive low-photon energies.

Finally, to improve the base pressure at the sample, we added a cryopump (ULVAC Cryogenic Inc., U8H) and an ion pump (ULVAC, PST-200CX2) to the photoemission chamber. As a result, we achieved the base pressure of 5×10^{-9} Pa better than before (2×10^{-8} Pa). For further improvement of base pressure, we plan to equip a thermal radiation shield around the sample in FY2009.

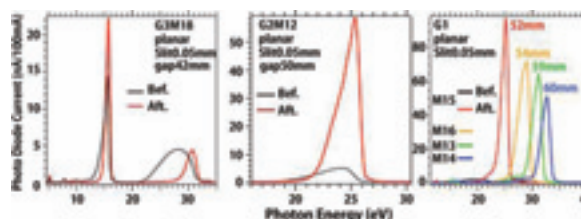


Fig. 1. Improvements of throughput spectra before and after the realignment of optics at BL7U.

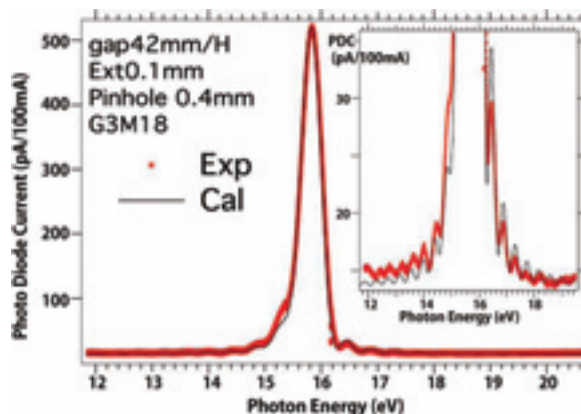


Fig. 2. Throughput spectrum at low photon-energy region in comparison with the calculation.

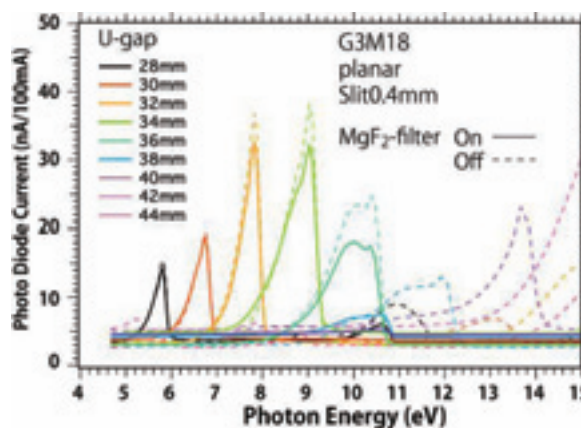


Fig. 3. Throughput spectra with some undulator gap size with and without a VUV filter, MgF_2 , in the low photon-energy region.

[1] S. Kimura *et al.*, AIP Conf. Proc. **879** (2007) 527.

Improvement of the SGM-TRAIN monochromator at UVSOR-II BL5U for low excitation-energy photoemission

T. Ito, H.J. Im*, S. Kimura, E. Nakamura

UVSOR Facility, Institute for Molecular Science, Okazaki 444-8585, Japan

*School of Physical Science, The Graduate University for Advanced Studies, Okazaki 444-8585, Japan

BL5U at UVSOR-II storage ring has been reconstructed in 2004's for high-resolution photoemission (HRPES) study for solids and surfaces [1]. The energy and angular resolutions of the photoemission apparatus constructed at the end-station of BL5U have been improved to $\Delta E \sim 1.2$ meV and $\Delta\theta \sim \pm 0.1^\circ$, which is sufficient to study the anomalous physical properties such as the metal-insulator transition, superconductivity, magnetic phase transition, *etc.* However, it has been hard to study the above properties at BL5U because of the old-type beamline designed in 1995's, in spite of the extensive improvement of the end-station and the storage ring [1,2]. Main problems interrupting a high-resolution study were as follows. (1) Mechanism for optimizing the front mirror was too rough to operate the focus position of the undulator light. (2) Entrance slit has no cooling system. (3) The grating G3 with normal incident mount for the low energy region ($h\nu = 5 - 25$ eV) has been optimized to the bending magnet radiation [3]. The above has caused the extremely low throughput at the low-energy region and restricted the HRPES experiment.

Taking account of the problems listed above, we have reconstructed the beamline in the following way to improve the efficiency in the PES experiment with using the low-energy photons at BL5U. (1) The mechanics at the front mirror was updated to the high-precision system controlled by the pulse-motors. (2) The water-cooling system was attached at the holder of the entrance slit. (3) The monochromator (SGM-TRAIN) was re-arranged to the optimum condition to the undulator light.

Figure 2 shows the improved throughput from the SGM-TRAIN monochromator after the present reconstruction. Comparing with the previous throughput spectra (Fig. 1), we can clearly find that the mesh current increases about 30 times higher, and the energy resolution becomes better because of the sharper interference from the optical klystron-type undulator as shown in Fig. 2. Due to the high-throughput of the photocurrent at the low-energy region, the HRPES measurement at BL5U becomes available. For example, HRPES spectrum at the Fermi-level of gold (Fig. 3) has been corrected within 1 hour with the resolution of $h\nu/\Delta E \sim 1000$. We believe that the present reconstruction makes it

possible to explore the origin of the anomalous physical properties by using the high-resolution bulk-sensitive angle-resolved photoemission apparatus at UVSOR-II BL5U.

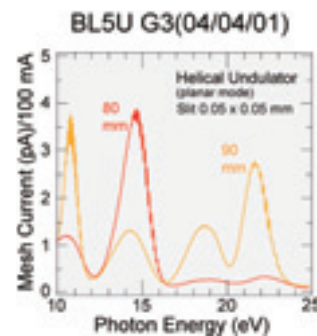


Fig. 1. Throughput spectra from the SGM-TRAIN monochromator with the normal incident grating G3 measured before the present reconstruction [1].

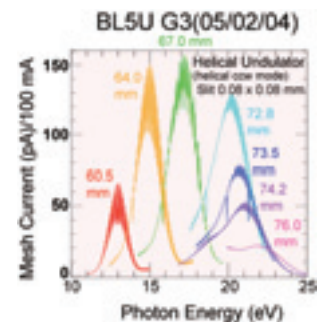


Fig. 2. Same as Fig. 1, but measured after the present reconstruction.

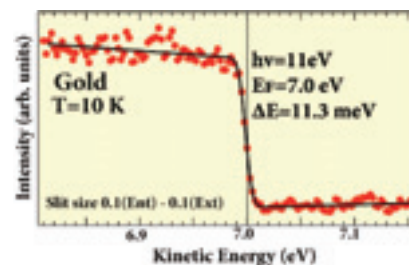


Fig. 3. HRPES spectrum at the Fermi level of gold measured after the present reconstruction.

- [1] T. Ito *et al.*, UVSOR Activity Report 2003, 40.
- [2] M. Katoh *et al.*, UVSOR Activity Report 2003, 5.
- [3] M. Kamada *et al.*, Rev. Sci. Instrum. **66**, 1537 (1995)

Development of Integrated Software for Beamline Control for Photoemission Beamlines at UVSOR-II

Masahiro Sakai,¹ Takahiro Ito,² Shin-ichi Kimura^{1,3}

¹*UVSOR Facility, Institute for Molecular Science, Okazaki 444-8585, Japan*

²*Graduate School of Engineering, Nagoya University, Nagoya 464-8603, Japan*

³*School of Physical Sciences, The Graduate University for Advanced Studies, Okazaki 444-8585, Japan*

We developed integrated software for synchronized motion of a beamline from the undulator light source to the photoemission end station. UVSOR-II, Institute for Molecular Science, has two photoemission beamlines with undulator light sources. One of the beamlines, BL7B, is dedicated for a high-resolution angle-resolved photoemission and equips an APPLE-II-type undulator (NEOMAX Co.), a Wadsworth-type 10-m normal-incidence monochromator (TOYAMA Co.), a 200-mm radius hemispherical photoelectron analyzer (MB Scientific AB, A-1), and a 6-axes manipulator with liquid-helium-cooled cryostat (R-dec Co., i-GONIO). [1] Another beamline, BL5U, also equips the same photoelectron analyzer. [2] In both beamlines, since the control PCs are spatially separated, the operability of the beamline has not satisfied. Then we developed a new multi-client server/client system using the TCP/IP protocol by the LabVIEW software. At present, absorption measurements where the undulator and the monochromator are controlled can be performed. Since the photoelectron analyzer and the manipulator are also controlled by the LabVIEW software, a constant initial state (CIS) measurement and a Fermi surface mapping will be automatically realized in the near future. In this paper, we report the present progress in the development.

[1] S. Kimura, T. Ito, E. Nakamura, M. Hosaka, M. Katoh, AIP Conf. Proc. **879**, 527 (2007).

[2] T. Ito, S. Kimura, H.J. Im, E. Nakamura, M. Sakai, T. Horigome, K. Soda, T. Takeuchi, AIP Conf. Proc. **879**, 587 (2007).

UVSOR Users Meeting

Place: Okazaki Conference Center

November 13, 2009

13:30-14:30

Opening Remarks

Preface

Present Status and Upgrade Plan of UVSOR Accelerators

Electronic Structure and Structure of Endohedral

Metallofullerenes by Photoelectron Spectroscopy

14:40 - 16:30

Photoluminescence and Photoluminescence Excitation Spectra
from AlN doped with Gd³⁺

Dependence of Reflectance and Responsivity of UV Detectors on
Angle of Incidence

Multiproduction by Hot Photocarriers Created in Inorganic EL
Phosphors

Luminescence of Rare Earth Ion doped Hydroxyapatites Excited
by UVSOR

Design for VIS-VUV Spectroscopic Beam Line BL3B

K. Fukui (Fukui Univ.)

N. Kosugi (UVSOR)

M. Katoh (UVSOR)

T. Miyazaki (Ehime Univ.)

S. Sawai (Fukui Univ.)

T. Saito (NMIJ, AIST)

M. Kitaura
(Yamagata Univ.)

M. Ohota (Niigata Univ.)

R. Ikematsu (Fukui Univ.)

16:30-18:00

Poster Session

18:15-

Banquet

November 14, 2009

9:00-10:20

Current Status of BL6U

Present Status of BL7U

Electronic Structure of Organic Thin Films and

Interfaces: Present Understanding and Future Prospects

10:30 - 12:00

Fragmentation of Fullerenes Induced by Extreme UV
Photoirradiation

Crystal Quality Evaluation of Superconducting InN by
Phonon-Polariton

Origin of the Valence Transition of SmS Revealed by Infrared
and Terahertz Spectroscopy at High Pressure and Low
Temperature

Effect of Temperature Dependent Chemical Potential on
Thermoelectric Power

Ferromagnetic Phase Transition and Electronic Structure of
EuO Thin Films

E. Shigemasa (UVSOR)

T. Ito (Nagoya Univ.)

H. Yamane (IMS)

K. Mitsuke (IMS)

T. Inushima (Tokai Univ.)

S. Kimura (UVSOR)

T. Takeuchi (Nagoya Univ.)

H. Miyazaki (UVSOR)

Poster Session

1. Luminescence Properties of CsI Crystals Activated with Ag⁻ and Au⁻ Ions
 2. XANES Spectra of Sulfur K-edge of Cystine
 3. Vacuum Ultraviolet Absorption Spectrum of DNA Bases and Examination of the Thomas-Reiche-Kuhn Sum Rule
 4. Absorption Cross Section of L-Methionine in Sulfur K-Edge Region
 5. Optical Oscillator Strength Distribution of Amino Acids in Ultra Vacuum Violet
 6. Photoelectron Spectroscopy of Pseudo-one Dimensional Ba₃Co₂O₆(CO₃)_{0.7}
 7. Optical Properties of YAG Ceramics Doped with Impurity Ions
 8. Strong Coupling Superconductivity in Iron-Based Superconductor Ba_{1-x}K_xFe₂As₂ Studied by High-Resolution ARPES
 9. Study of Local Structure of SiO₂-Hydroxyapatite by Hydrothermal Process
 10. In Situ Observation of Photostructural Changes in Amorphous Semiconductor by Total Photoyield
 11. Local Structure of Mg in ZrO₂ for Alternative Joints with High Biocompatibility
 12. Electronic Structure of Mn₃Cu_{1-x}Ga_xN Studied by Ultraviolet and Soft X-Ray Photoemission
 13. Design for VIS-VUV Spectroscopic Beam Line BL3B
 14. Electronic Structure of Mn₃Cu_{1-x}Ga_xN Studied by Ultraviolet and Soft X-Ray Photoemission
 15. Polarization Properties of Optical Reflectance, Photoluminescence and Photoluminescence Excitation Spectra from AlN
 16. Photoluminescence and Photoluminescence Excitation Spectra from AlN Doped with Gd³⁺
 17. Reflection Measurement on Si/W/Co and Si/W/C Multilayers for Use in 50–110 nm Region
 18. Study of the Magnetic Film Formed on the Si Substrate with Passivation Layer
 19. Electronic Structure Analysis of Mn and Fe Ions in In₂O₃
 20. XANES Analysis of Electronic Structure of Mn in Pr_{1-x}A_xMnO_{3-δ} (A=Ca, Sr)
 21. Amounts of Electron Transfer in Tm-Entrapped Metallofullerens
 22. Electronic Structure of Sulfur-Containing Organic Solid with High Mobility
 23. UVSOR Accelerators Upgrade Plan in Spring of 2010
 24. Generation of Ultra-Short Gamma-ray Pulses by Laser Compton Scattering in an Electron Storage Ring
 25. Status of Top-Up Operation at UVSOR-II
 26. Present Status of UVSOR-II Free-Electron Laser
 27. Pressure-Dependent IR/THz Reflectivity Spectra of CeIn₃
 28. Current Status of Coherent Harmonics Light Source in UVSOR-II
 29. Three-Dimensional Angle-Resolved Photoemission Spectroscopy of EuO Thin Films
 30. Present Status of THz Coherent Light Source Development
 31. Ce 4d-4f Resonant Angle-Resolved Photoemission Study of Heavy-Fermion Systems in Weakly Hybridized Regime
 32. Decomposition and Chirality Formation of Amino Acids by CP-UVL Irradiation
- T. Kawai (Osaka Pref. Univ.) et al.
M. Tabe (Kobe Univ.) et al.
A. Mimoto (Kobe Univ.) et al.
Y. Izumi (Kobe Univ.) et al.
A. Imazu (Kobe Univ.) et al.
K. Soda (Nagoya Univ.) et al.
H. Uno (Gifu Univ.) et al.
K. Nakayama (Tohoku Univ.) et al.
K. Nakata (Osaka Pref. Univ.) et al.
K. Hayashi (Gifu Univ.)
T. Monden (Osaka Pref. Univ.) et al.
Y. Miyata (Ritsumeikan Univ.) et al.
R. Ikematsu (Fukui Univ.) et al.
K. Ozaki (Fukui Univ.) et al.
T. Ito (Fukui Univ.) et al.
S. Sawai (Fukui Univ.) et al.
M. Watanabe (Shanghai Dianji Univ.) et al.
Y. Takagi (IMS) et al.
T. Okazaki (Waseda Univ.) et al.
H. Kanamori (Waseda Univ.) et al.
Y. Tokumoto (Ehime Univ.) et al.
T. Zaima (Ehime Univ.) et al.
J. Yamazaki (UVSOR) et al.
Y. Taira (Nagoya Univ., UVSOR) et al.
K. Hayashi (UVSOR) et al.
H. Zen (UVSOR) et al.
T. Iizuka (SOKENDAI, UVSOR) et al.
T. Tanikawa (SOKENDAI, UVSOR) et al.
H. Mitani (Shinshu Univ., UVSOR) et al.
M. Adachi (UVSOR) et al.
H. J. Im (Hirosaki Univ.) et al.
S. Shima (Yokohama National Univ.) et al.

Status and Prospects of Synchrotron Light Source Technologies

Feb. 19, 2010

Room 301, IMS Research Facilities Building

12:55	Opening Remark	M. Katoh (UVSOR)
13:00	Status of UVSOR-II	M. Katoh (UVSOR)
13:30	Status of HiSOR	K. Gotoh (HiSOR)
14:00	Status of PF/PF-AR	T. Honda (KEK)
14:30	Status of KEK-ERL Project	M. Shimada (KEK)
15:00	Coffee Break	
15:15	Top-up Operation at PF	K. Harada (KEK)
15:45	Top-up Operation at UVSOR-II	H. Zen (UVSOR)
16:15	Top-up Operation at New SUBARU	Y. Shoji (New SUBARU)
16:45	Coffee Break	
17:00	Beam Injection with Pulsed Multi-Pole Magnet at PF	H. Takagi (Tokyo Univ.)
17:30	Status and Prospects of Beam Feedback Technologies	M. Tobishima (KEK)
18:00	Dust-Trapping at PF-AR	Y. Tanimoto (KEK)
18:30	UVSOR Facility Tour	
19:00	Banquet at UVSOR	

Feb. 20, 2010

9:00	Beam Diagnostics at PF	T. Obina (KEK)
9:30	Status of Visible Light Beam Line and Beam Diagnostic Beam Line at SPring-8	K. Tamura (SP8/JASRI)
10:00	Performance Characteristics Measurements of X-Ray Streak Camera at SPring-8	A. Mochihashi (SP8/JASRI)
10:30	Beam Diagnostics with Electronic Scheme at SPring-8	T. Fujita (SP8/JASRI)
11:00	Coffee Break	
11:15	Status of Light Source Developments at UVSOR-II	M. Adachi (UVSOR)
11:45	Status and Prospects of SAGA-LS	S. Koda (SAGA-LS)
12:15	Status of Central Japan Synchrotron Radiation Research Facility and Light Source Accelerator	N. Yamamoto (Nagoya Univ.)
12:45	Closing Remark	T. Kasuga (KEK)



Editorial Board

M. Adachi

H. Hagiwara

M. Masuda

H. Zen